

EgoProx: Evaluating MLLMs on Egocentric 3D Proximity Reasoning Across a Cognitive Hierarchy

Jinzhao Li^{1,2}, Yinuo Chen^{1*}, Dongxu Piao^{1*}, Panwang Pan^{2†}, Yifan Yu², Dong Wang², Honglei Yan², Liang Yue¹, Shaofei Wang³, Yixin Chen³, Siyuan Huang³, Miao Liu^{1‡}

¹College of AI, Tsinghua University

²ByteDance

³State Key Laboratory of General Artificial Intelligence, BIGAI

<https://lijinzhao30.github.io/Egoprox/>

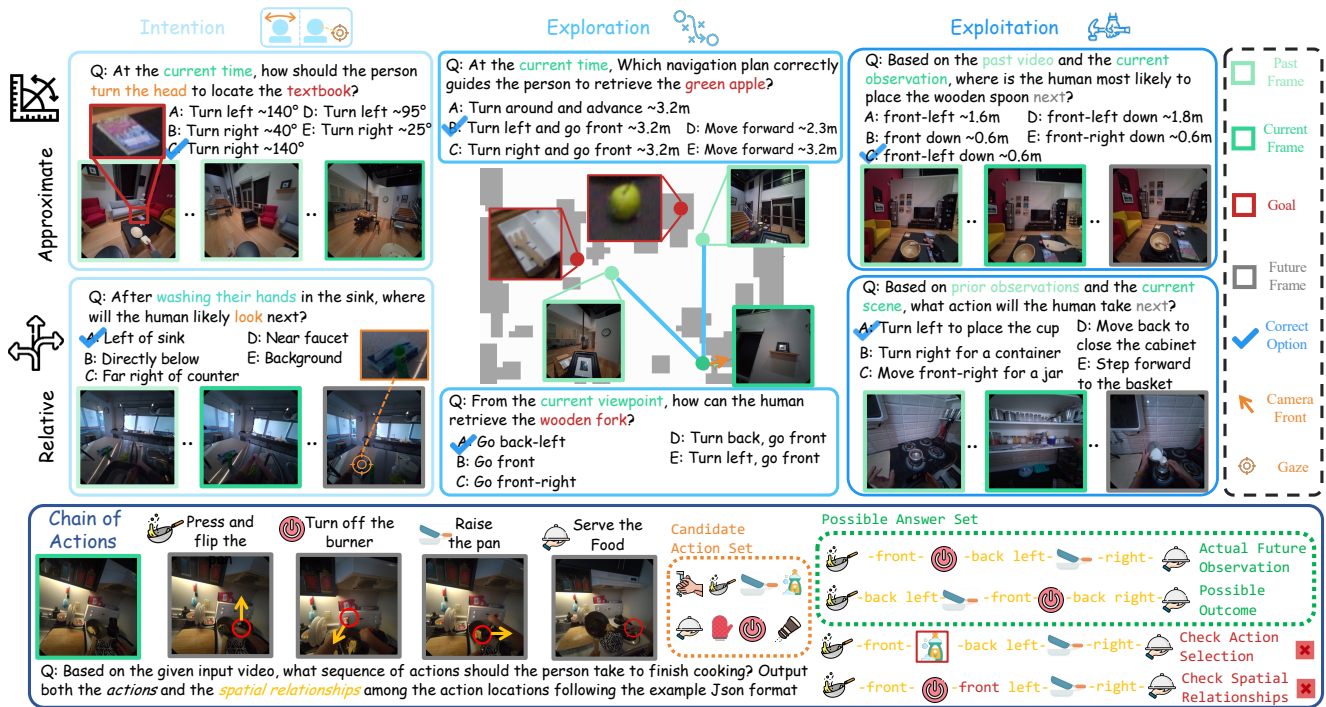


Figure 1. **Visual illustration of the EgoProx benchmark.** We aim to evaluate multimodal large language models (MLLMs) on complex egocentric proximity reasoning tasks that require 4D action and scene understanding. Our benchmark spans four core dimensions following a cognitive hierarchy: Intention, Exploration, Exploitation, and Chain of Actions. We adopt approximate transformations and relative spatial relationships to represent proximity. The examples illustrate the model’s need to interpret long-term contextual cues, spatial dependencies, and action-state changes from first-person visual inputs, providing a comprehensive assessment of egocentric spatial intelligence.

Abstract

Humans constantly reason about 3D proximity, the relations between their body and surrounding objects, to guide perception and action in daily life. Whether multimodal large language models (MLLMs) can perform such embodied 3D reasoning remains unclear. To this end, we intro-

duce **EgoProx**, a benchmark for egocentric 3D proximity reasoning. We organize our tasks along a cognitive chain, covering intention, exploration, exploitation, and chain-of-actions reasoning. We also design an agent based data engine that produces diverse and consistent QA pairs at scale. We benchmark prevailing MLLMs on EgoProx and conduct additional analyses with dataset specific and task specific instruction tuning. We observe large cross-domain gains, indicating that current MLLMs contain some spatial knowl-

*Equal contribution. † Project Lead. ‡ The corresponding author.

edge; however, they still struggle to effectively leverage it for spatial reasoning VQA.

1. Introduction

Humans constantly reason about 3D proximity, the spatial relations between their body and nearby objects in everyday life. Through 3D spatial awareness, the cognitive system drives intention such as head orientation and gaze shifts, leading to coordinated motor behaviors like locomotion and reaching, which further support hierarchical interactions in complex 3D scenes [7]. This 3D reasoning capability is a key mechanism that connects perception and actions. However, despite rapid advances in multimodal large language models (MLLMs) [2, 4, 10, 12, 15, 17, 26, 29, 33, 35, 36, 39, 47, 54, 58, 60, 62, 65, 76, 85], it remains unclear whether current systems can emulate this human spatial reasoning within 3D scenes.

Egocentric video offers a natural lens for studying this problem. Its first-person viewpoint, embodiment, and continuous streaming reveal how humans form intentions through preparatory cues such as gaze and head motion, explore their surroundings, exploit spatial affordances, and ultimately coordinate chains of actions within 3D space [1, 40, 41, 45, 50]. An MLLM capable of reasoning about spatial proximity from the user’s perspective holds strong potential for applications in smart glasses, augmented reality, and robotics [59, 78].

However, despite the growing interest in egocentric MLLMs [22, 30–32, 38, 44, 46, 52, 56, 57, 63, 70, 72, 79], 3D proximity reasoning remains unexplored in existing egocentric visual question answering benchmarks. Establishing such a benchmark is essential to advance research in embodied spatial intelligence and to enable more capable AI systems. To this end, we introduce **Egocentric Proximity Reasoning (EgoProx)**, the first benchmark for assessing whether MLLMs can model the 3D perception–action coupling from a first-person perspective.

Here, we draw an analogy to the exploration and exploitation trade-off in machine learning. Unlike machine learning systems that must balance between exploration and exploitation, the egocentric viewpoint inherently captures how humans both explore and exploit the 3D world within a unified perceptual stream, while simultaneously encoding intention as the driver of embodied behavior. Consequently, we characterize 3D proximity reasoning along a cognitive hierarchy comprising three domains: *intention*, *exploration*, and *exploitation*. As for the proximity measurements, we consider *approximate proximity*, capturing metric transformations such as translation and rotation, and *relative proximity*, describing spatial relationships between entities. Both reflect how humans naturally perceive spatial awareness. We further introduce a *chain-of-actions* set-

ting that extends our benchmark to assess higher-order cognitive processes underlying continuous human behavior in complex 3D scenes. We provide a visual illustration of our benchmark in Fig. 1.

A key challenge in constructing such a benchmark is designing a semi-automatic pipeline that supports VQA data generation. Unlike prior VQA benchmarks that rely on MLLMs with human-in-the-loop refinement [22, 43], existing models lack the spatial intelligence to produce high-quality question–answer pairs [4, 39, 76, 78, 85]. Moreover, our diverse set of tasks require different reasoning capabilities, making a single foundation model insufficient. To address this, we develop an agent-based data engine that orchestrates multiple specialized tools to generate high-quality VQA data across diverse task types. Our agentic data engine tailors its workflow to the data generation requirements of each task type in our benchmark, it first applies the salient clip sampler to extract informative segments from long egocentric videos, and then selects and composes the appropriate tools from the 3D analysis toolset to complete VQA generation. Our key contributions are summarized as follows:

- We propose EgoProx, the first benchmark designed to evaluate whether MLLMs can reason 3D perception–action coupling from an egocentric point-of-view, with four tasks organized along a cognitive hierarchy: Intention, Exploration, Exploitation, and Chain of Actions.
- We develop an agent-based data generation pipeline that leverages task-aware salient clip sampler and 3D analysis toolset to automatically synthesize high-quality VQA data across diverse task categories.
- Through extensive evaluation and cross-domain instruction-tuning experiments, we demonstrate that existing MLLMs already contain latent spatial knowledge acquired during pretraining, but unlocking this capability requires structured supervision.

2. Related Work

Egocentric VQA Benchmark. There has been a growing interest in developing benchmarks that systematically evaluate the spatial reasoning capabilities of multimodal large language models (MLLMs) [55]. Most existing benchmarks [3, 37, 71, 73] formulate spatial reasoning VQA tasks using image sequences derived from 3D scans or manually curated by researchers. Therefore, these works are largely limited to object- or scene-centric geometric reasoning and overlook whether MLLMs can understand 3D proximity in everyday human activities from a user-centric perspective, as explored in our proposed EgoProx benchmark. A few egocentric VQA benchmarks have been proposed to evaluate models’ ability to reason about first-person behaviors [14, 43, 83, 83]. EgoSchema [43] introduces visual question answer pairs to test causality understanding of ego-

centric narratives. EgoPlan [11] focuses on goal-oriented reasoning from ongoing activities. Peng et al. [51] further developed a VQA benchmark that evaluates egocentric gaze-informed reason. Huang et al. [25] introduced EgoDynamics4D, which targets for 3D object- or agent-centric grounding. Although these works share a similar motivation toward human-centric perception and behavior understanding, our benchmark is the first to evaluate the cognitive reasoning of **3D proximity** during daily activities.

Egocentric Multimodal Foundation Models. MLLMs have achieved remarkable progress in exocentric contexts [2, 4, 10, 12, 17, 35, 36, 39, 47, 54, 62, 62]. Nevertheless, the substantial domain gap between exocentric and egocentric visual-language data [32] greatly limits the generalization of exocentric-trained models when applied to first-person scenarios. Recent advances in egocentric multimodal learning have introduced specialized pretraining paradigms that explicitly align vision and language representations from a first-person perspective. Egocentric captioning benefits from cross-view or instructional adaptation strategies [46, 70], while question answering evolves toward temporally grounded reasoning [22, 63]. Kurita et al. [31] and Sun et al. [57] extend language grounding to dynamic, interaction-rich scenes. Moreover, language-guided action generation and instruction following [32, 44] connect egocentric observation with embodied decision-making. The pioneering EgoVLP [38] and EgoVLPv2 [52] conducted large-scale video-language pretraining using Ego4D narrations. Zhao et al. [79] and Suglia et al. [56] refined visual-language alignment for long egocentric video understanding. More recently, Yang et al. [72] proposed an omnimodal system that integrates models such as EgoGPT and EgoRAG to unify perception, reasoning, and interaction for egocentric understanding, while GazeGPT [30] augmented large MLLMs with additional inputs to improve contextual reasoning for smart eyewear. Despite these advancements, existing egocentric MLLMs remain limited in addressing 3D spatial reasoning, underscoring the importance of our proposed EgoProx Benchmark.

Spatial Intelligence. Recent studies have suggested that existing multimodal large language models (MLLMs) still exhibit limitations in spatial intelligence [8, 21], motivating growing efforts to enhance this capability [8, 16, 19, 21, 68, 80]. Prevailing methods have attempted to directly encode 3D information such as point clouds [9, 19, 21], multi-view images [21, 84] and objects [9, 23, 24, 64] as the context of MLLMs, following the footsteps of vision-language models (VLMs) to bridge the gap between 3D and language representations. Another line of work aims to enhance the spatial reasoning capabilities of MLLMs using only 2D inputs, such as images [8, 16] or videos [53, 68]. Chen et al. [8] proposed SpatialVLM, which leverages well-developed 3D computer vision techniques such as monocular depth es-

timation, semantic segmentation, and region captioning to extract 3D spatial information from 2D images, using it as QA pairs to train MLLMs for spatial understanding. The Spatial-MLLM proposed by Wu et al. [68] effectively encodes keyframes from videos into 3D information by incorporating the VGGT [61] backbone, which is then fused with 2D embeddings before being input into MLLMs. Our benchmark also aims to evaluate the spatial reasoning capabilities of MLLMs without relying on explicit 3D representations as auxiliary modalities. This design choice aligns with the observation that humans can naturally infer approximate 3D proximity and spatial relationships from purely 2D visual inputs.

3. EgoProx Benchmark

In this section, we first introduce the formal definitions of the four task categories in our proposed EgoProx benchmark. We then describe the data sources and highlight the key features of the benchmark.

3.1. Task Definition

We categorize proximity reasoning tasks along a cognitive hierarchy: human *intention* shifts toward intermediate goals, driving both *exploration* and *exploitation* of the 3D environment. In addition, we include a more challenging *chain-of-actions* reasoning task, which requires models to infer the multi-step proximity reasoning process underlying complex actions.

Formally, we define input video segments $\mathcal{X} = \{x_1, x_2, \dots, x_T\}$, where T is the total number of frames, x_T denotes the current frame, and x_1, \dots, x_{T-1} represents the past frames. Each task examines the ability of the model f_θ to infer the correct answer \mathcal{A} from a discrete set of candidates \mathcal{C} , given a natural language question \mathcal{Q} and \mathcal{X} .

Exploration evaluates whether f_θ can predict the navigation step \hat{s} toward the goal G , with the goal specified by the query Q and visible within the input video segment \mathcal{X} .

Exploitation assesses whether f_θ can predict how the next human-object interaction \hat{h} will happen in 3D space, given the observable segment \mathcal{X} and the query Q describing the ongoing manipulation context.

Intention examines whether f_θ can predict immediate body movements \hat{m} , including gaze shifts or head movements conditioned on the goal G specified by the query Q , based on the observable segment \mathcal{X} .

Chain-of-Actions Reasoning assesses whether f_θ can predict a sequence of future actions $\{a_1, a_2, \dots, a_K\}$ and their relative spatial relationships $\{e_i\}$ of action locations, given the observable segment \mathcal{X} , a high-level goal G , and the query Q . Specifically, each e_i encodes the spatial relation between consecutive locations (l_i, l_{i+1}) , using the image plane of frame x_T as the reference coordinate. We also provide number of steps k and a candidate action set \mathcal{S} con-

sisting of the future actions a_1, \dots, a_k along with a set of distraction actions to limit the exploration space of MLLMs.

When designing the correct answer \mathcal{A} and the distractor options, we consider two types of proximity measurements: (1) *Approximate proximity*, which encodes coarse metric transformations required at the last observable time step T , parameterized by angular rotations and translational displacements; and (2) *Relative proximity*, which represents discrete spatial relationships between a reference and a target entity at time T , characterized by spatial predicates (e.g., left–right, front–back, near–far) that describe directional topology rather than absolute metric distance. Considering the challenging nature of the Chain-of-Actions task, we evaluate only the relative proximity for this task.

3.2. Data Source

To construct our benchmark, we leverage the existing EgoExo4D [20] and Aria Digital Twin (ADT) [49] datasets. Both capture egocentric video streams from fisheye cameras, along with calibrated poses and eye-tracking data. EgoExo4D provides upper-body pose annotations and atomic action descriptions but lacks 3D object annotations, whereas ADT offers dense 3D object annotations but lacks semantic action labels. Activities in EgoExo4D often occur in constrained environments with limited locomotion, making it unsuitable for exploration-related reasoning. In contrast, activities in ADT mainly involve walking within the scene and manipulating objects but lack goal-oriented behaviors, making it inadequate for chain-of-actions reasoning. The detailed distribution of benchmark data sources is provided in the Supplementary Materials.

3.3. Benchmark Characteristics

As shown in Table 1, we provide a detailed comparison between our EgoProx and related benchmarks in egocentric vision and spatial intelligence. Our EgoProx encompasses a broad spectrum of reasoning tasks and represents the first benchmark to assess 3D spatial intelligence in the context of human behavior. While most existing VQA benchmarks categorize tasks by reasoning type (e.g., grounding, planning, forecasting), we instead characterize our dataset according to the cognitive hierarchy as introduced earlier. This design choice stems from the coupled nature of intention perception and action execution in egocentric videos. It is worth noting that the question types in our benchmark still resonate with prior efforts. As detailed in Sec. 3.1, the Intention, Exploration, and Chain of Actions categories evaluate a model’s ability to infer subsequent steps based on the current state, thereby aligning closely with grounding and planning tasks. In contrast, the Exploitation category assesses the model’s ability to predict short-horizon or intermediate future events, corresponding to the forecasting dimension defined in existing benchmarks. Notably, such

Table 1. Comparison of EgoProx with existing 3D reasoning VQA or egocentric activity VQA benchmarks. We summarize key properties including 3D awareness, dataset scale, reasoning types, construction methodology, and temporal reasoning range. The reasoning types include grounding (G), forecasting (F), planning (P), and causality (C). Benchmark construction types include human annotation, MLLM/LLM-based generation, and agent-based generation. For clarity, note that human review for quality assurance is adopted by all existing QA-generation pipelines, including ours.

	Benchmark	3D Space	# of Samples	Reasoning Type	Construction	Temporal Range
No Action	ScanQA[3]	✓	46313	Grounding	Human	Short
	MMSI-Bench[73]	✓	1000	Grounding	Human	Short
	VSI-Bench[71]	✓	5000+	Planning	Human	Short& Long
	OST-Bench[37]	✓	10k	Grounding	Human	Short
	OpenEQA[42]	✓	1600+	Grounding	Human	Short
	VLM4D[82]	✓	1800+	Grounding	Human	Short
Egocentric Action	EgoVQA[18]	✗	581	Grounding	Human	Long
	EgoTextVQA[83]	✗	7064	Grounding	MLLM	Short& Long
	EgoMemorial[75]	✗	7026	Grounding	LLM	Short& Long
	QAEgo4D[6]	✗	1854	Grounding	Human	Short& Long
	AssistQ[67]	✗	531	Grounding	Human	Long
	Ego-ST[69]	✓	5000+	G&P	Human	Long
	EgoDynamics4D[25]	✓	927K	Grounding	MLLM	Short& Long
	EgoThink[14]	✗	700	G&F&P	Human	Short
	EgoTaskQA[28]	✗	40K	Grounding	LLM	Short
	EOE-Bench[77]	✗	3277	G&F	Human	Short
	VideoMindPalace[27]	✗	1757	Grounding	MLLM	Short& Long
	EgoGazeVQA[51]	✗	1800	G&C	MLLM	Short
	EgoSchema[43]	✗	5063	Causality	LLM	Long
	EgoPlan[11]	✗	4939	Planning	MLLM	Long
	EgoLifeQA[72]	✗	6000	Grounding	LLM	Long
EgoProx (Ours)	✓	2405	G&F&P	Agent	Short& Long	

a comprehensive benchmark requires a carefully designed data construction pipeline, even when leveraging datasets like EgoExo4D and ADT that already include valuable annotations and modalities.

4. Agentic Data Engine

As shown in 2, given an egocentric video, along with its associated metadata (camera pose, objects and action labels etc.), and a user-specified question category, our agent uses Gemini-2.5-Pro as the foundation and orchestrates a suite of specialized tools to synthesize question–answer pairs in a controllable manner. We introduce the key components of our agent in the following sections.

4.1. Salient Clip Sampler

The first step of our data engine is to extract an ideal clip $\mathcal{X} = \{x_1, \dots, x_T\}$ from a long egocentric video. Although datasets such as EgoExo4D provide coarse temporal annotations, our tasks require finer alignment to ensure that each question is answerable from the last observable frame x_T . We therefore adopt a unified sampling principle that organizes all tasks into two functional categories. Forecasting tasks, such as gaze forecasting in *Intention* and next-interaction prediction in *Exploitation*, are defined by future supervisory events. We detect the moment where a stable gaze fixation or a human–object interaction occurs, and then select the video segment preceding this event so that $\{x_1, \dots, x_T\}$ implicitly encodes the preparatory cues leading into the upcoming behavior. Planning tasks, including head-orientation reasoning in *Intention*, *Exploration*, and

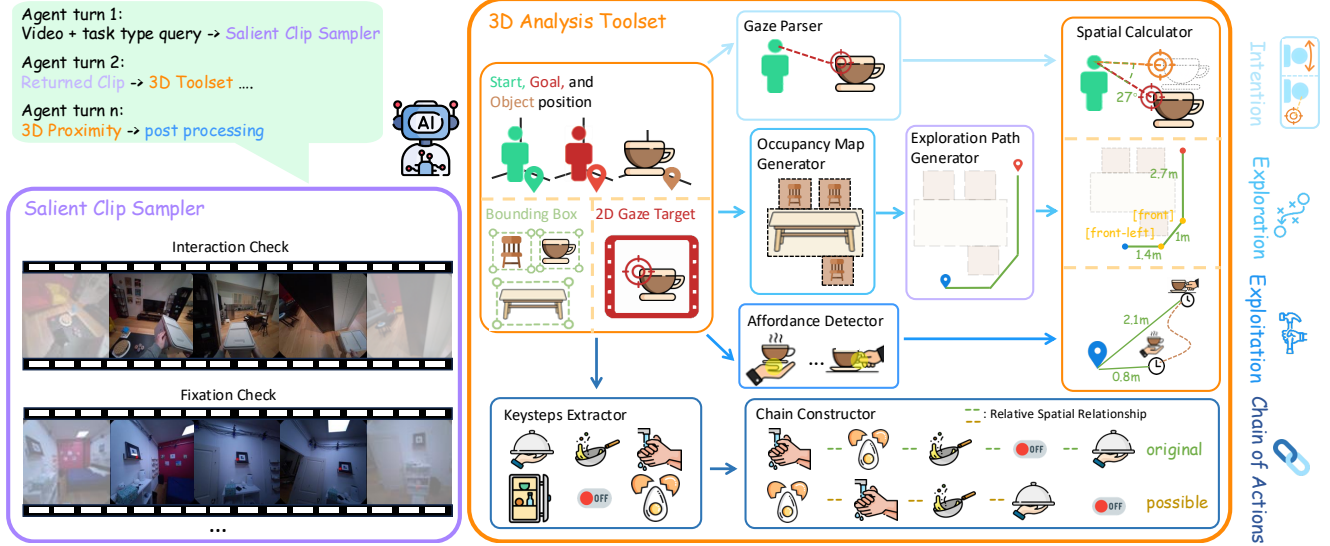


Figure 2. **Overview of our agent-based data construction pipeline.** The agent first identifies salient moments with an interaction- and fixation-based sampler, then uses the 3D Analysis Toolset to extract spatial cues such as object positions, gaze targets, occupancy maps, and action chains. It then invokes the Spatial Calculator to derive 3D distances, orientations, and proximity relations, producing structured 3D proximity ground truth. Final benchmark question-answer pairs are compiled through necessary post-processing.

Chain of Actions tasks, require clips that provide partial but sufficient evidence for achieving a given goal G . For Exploration and head-orientation reasoning, we enforce that G is visible in some earlier frame x_t but not in the final observation x_T , determined through field-of-view visibility checks. For Chain of Actions, we identify dense regions of keysteps, derive a high-level goal from the earlier portion of the window, and ensure that several future steps remain after x_T so that the multi-step plan is still inferable. This task-driven clip sampler guarantees that each extracted video segment contains the minimal yet sufficient cues required for the intended form of 3D proximity reasoning.

4.2. Toolset for 3D Analysis

In Fig. 2, we provide a visual illustration of our toolsets and how they are used to construct the ground truth for the four task categories. We briefly introduce the input and output of each tool here, with implementation details provided in the Supplementary Materials.

Occupancy Map Generator constructs an occupancy map from the 3D bounding boxes associated with \mathcal{X} , identifying free or occupied regions for obstacle checking.

Exploration Path Generator computes a feasible path within the occupancy map from the query position to the goal position using an 8-connected A* search algorithm. Note that for navigation step generation, we do not use the actual camera trajectory to derive this path, as human motion is inherently stochastic and poses significant challenges for MLLMs to interpret reliably.

Spatial Calculator consists of the Distance Calculator and

the Direction Calculator. The Distance Calculator projects both camera and object positions into a unified world coordinate system and computes the translation distances between the queried entities. While the Direction Calculator returns the angle between the camera’s forward direction and the vector from the camera position to the target G , projected onto the Bird’s-eye View (BEV).

Gaze Parser transforms eye-tracking data from the 2D image plane into a corresponding 3D gaze ray, which is then used to localize the object being fixated.

Affordance Detector determines whether the target object G is interacted with in the future frames, and further computes, in the current frame \mathcal{X}_T , the direction and distance from the observer to G using aforementioned direction and distance calculators.

Keystep Extraction Tool returns the textual keysteps including the interactive objects, the observer, and the interaction names in the observation video.

Chain Constructor obtains possible chains of steps and the direction between the steps. First, the chain tool calculate the directions between the steps. Regarding it as the basically correct chain, the tool provides several possible correct chains using multi-modal large language models.

4.3. Toolset Usage

In a nutshell, the 3D proximity ground truth for a given input clip sampled for each task type is constructed as follows:

- **Intention:** The agent invokes the Spatial Calculator to estimate how the camera wearer adjusts head orientation toward the goal or directs gaze inferred by the Gaze Parser.

- **Exploration:** The agent samples a valid goal G based on visibility checks and adopts the Occupancy Map Generator and Exploration Path Generator to obtain a path composed of steps \hat{s} , each providing the distance and discrete direction for exploration.
- **Exploitation:** The agent utilizes an affordance detector to identify which part of the object G the observer is grasping in the anticipation frame, where the observer will place the object G , and which direction the observer will move to interact with the object G .
- **Chain of Actions:** Specifically, the agent employs the Keystep Extractor to extract key action steps and their 3D spatial locations from long video segments, and to identify the key actions toward the common goal G based on future observations. It then employs an LLM to construct a set of all possible ordered combinations of key steps leading toward the same goal. Finally, The agent calls the Chain Constructor to generate a complete set of possible answers by calculating the spatial relationships among the ordered combinations of key steps.

4.4. Post-Processing

As mentioned in Sec. 3.1, the proximity measurements include both approximate transformation and relative relationships. We discretize the transformation into intervals that are interpretable by humans. For spatial relationships, we convert the 3D directions into eight discrete orientations projected onto a specified plane. When constructing the candidate sets, we prompt the VLM to generate hard-negative distraction options. However, we provide specific instructions to ensure that these distractions do not rely on minor differences that are unsolvable even for humans.

We also conduct careful human verification to ensure both the answerability and accuracy of the ground truth. For the *Chain of Actions* task, we perform a thorough examination of all possible answer sets generated by the agent.

5. Experiments

5.1. Metrics

The majority of our benchmark consists of multiple-choice questions; therefore, we adopt a straightforward accuracy metric with a 20% chance level.

For the Chain of Action reasoning evaluation, we explicitly structure model outputs as a chain of nodes defined in 3.1, where each node represents a selected action step and the edge values encode their relative spatial relationships. In our benchmark, each sample consists of 3–5 steps, and the candidate action set \mathcal{S} contains 10 candidates. And our agent generates a ground-truth answer set \mathcal{Y} that encompasses all valid possibilities, and the size of the valid ground-truth set \mathcal{Y} ranges from 1 to 3. The Action Accuracy (*Act-Acc*) is computed by comparing the predicted ordered

nodes o_1, \dots, o_k with those in the ground-truth set.

For correctly predicted sequences, we further evaluate the spatial relationship accuracy, denoted as Relational Accuracy (*Rel-Acc-S*), defined as $c/(k-1)$, where c is the number of correctly predicted relationships and $(k-1)$ is the total number of edges. To account for ambiguity in action locations, we also introduce a relaxed version, Relational Accuracy–Loose (*Rel-Acc-L*), where a predicted orientation (e.g., front-right) is considered correct if the ground truth belongs to one of its adjacent directions (e.g., front, right, or front-right).

5.2. Results on EgoProx Benchmark

We first evaluate prevailing proprietary API-based models, including GPT-5 [48] and Gemini-2.5-Pro [17], as well as several recent open-source models, such as LLaVA-NEXT-Video-7B [34], MiniCPM-V 2.6 [74], InterVL 2.5 [13], and the Qwen-VL series [5] across different model scales. For all models, we use a unified inference model to ensure a fair comparison. The prompt specifies the task and response constraints, includes the question text, and provides a minimal output-format exemplar to enable deterministic parsing. We also employ a zero-shot reasoning-style prefix [66] that encourages step-by-step inference. We provide the exact prompt template in the Supplementary Materials.

We provide detailed experimental results in Tab. 2. Consistent with previous finds [73], even the most advanced proprietary models still struggle with 3D proximity reasoning compared to human-level capability. Particularly, humans perform consistently well on the Chain of Actions task, but MLLMs drop sharply relative to other tasks, highlighting the difficulty of long-horizon reasoning. Proprietary models slightly outperform their open-source counterparts, particularly on exploration tasks, likely due to large-scale pretraining corpora that include long video sequences demonstrating how agents traverse complex environments. In addition, the Qwen-VL series achieves the strongest overall performance among open-source models. However, unlike general VQA benchmarks, scaling up model size yields only limited performance gains, a trend consistent with recent findings in 3D spatial understanding VQA benchmarks [37, 73].

In this context, we pose a critical question: does the limited performance of existing models indicate an inherent absence of spatial intelligence, or does it instead reflect their inability to utilize the spatial knowledge implicitly encoded within their large-scale parameters when addressing spatial reasoning queries? In the following section, we conduct additional experiments to further investigate this question.

5.3. Additional Analysis

Hypothesis. Existing MLLMs should have gained latent spatial knowledge during pretraining, as the massive mul-

Table 2. Evaluation results of prevailing MLLMs on the EgoProx benchmark, where best scores are colored with **red** and the second best scores are colored with **orange**. All models are evaluated using a unified prompt that defines the egocentric, world, and image-plane coordinate systems, and adopts zero-shot chain-of-thought prompting following [66].

Model	Intention		Exploration		Exploitation		Chain of Actions		
	Approx.	Relative	Approx.	Relative	Approx.	Relative	Act-Acc	Rel-Acc-S	Rel-Acc-L
Human Level	62.50	75.33	60.00	63.15	82.02	85.25	80.23	63.25	83.12
<i>Proprietary Models</i>									
Gemini-2.5-Pro	42.75	37.13	36.90	29.32	50.24	45.17	25.14	17.03	52.36
GPT-5	33.16	40.35	41.18	34.55	46.45	45.17	21.74	20.83	52.71
<i>Open-source Models</i>									
LLaVA-NeXT-Video-7B	23.06	27.19	18.72	23.56	31.04	29.29	1.09	16.67	33.33
MiniCPM-V 2.6	28.50	29.24	22.99	9.42	37.44	31.60	2.63	25.00	50.00
InternVL 2.5-8B	26.94	28.95	18.72	19.37	36.02	33.77	8.25	6.25	52.08
Qwen2.5-VL-7B	33.68	29.24	27.27	20.42	38.63	34.34	5.98	2.27	46.21
Qwen2.5-VL-32B	31.35	33.92	30.48	17.80	45.97	40.55	10.33	7.02	45.61
Qwen2.5-VL-72B	30.83	35.38	29.41	24.08	46.21	40.26	13.04	14.24	48.61
Qwen3-VL-235B	34.46	33.33	28.34	27.75	45.97	42.28	10.87	11.67	51.25
Qwen3-VL-Plus	26.42	34.21	20.32	21.47	48.34	42.28	10.87	7.50	41.67

Table 3. Cross-category experimental results where best scores are colored with **red**. We leverage extra training data from one category generated by our data engine and evaluate performance across all categories. The additional data not only improves performance within the source category but also enhances cross-category generalization, revealing the inherent hierarchical structure of human cognition.

Model	Intention		Exploration		Exploitation		Chain of Actions		
	Approx.	Relative	Approx.	Relative	Approx.	Relative	Act-Acc	Rel-Acc-S	Rel-Acc-L
Qwen2.5-VL-7B	33.68	29.24	27.27	20.42	38.63	34.34	5.98	2.27	46.21
Qwen2.5-VL-7B + Intention Tuning	–	–	32.09	24.61	64.93	39.11	3.80	0.00	14.29
Qwen2.5-VL-7B + Exploration Tuning	45.34	35.09	–	–	45.26	34.34	7.61	14.29	40.48
Qwen2.5-VL-7B + Exploitation Tuning	56.48	36.55	27.27	20.42	–	–	4.35	0.00	16.67

Table 4. Cross-dataset experimental results. Fine-tuning on one dataset improves proximity reasoning on the other.

Model	ADT Evaluation		
	Intention	Exploration	Exploitation
Qwen2.5-VL-7B	35.94	23.81	47.64
EgoExo4D Only Tuning	48.70	27.78	64.57
Model	EgoExo4D Evaluation		
	Intention	Exploration	Exploitation
Qwen2.5-VL-7B	26.74	–	32.52
ADT Only Tuning	50.58	–	43.67

timodal data consisting of image–text pairs, video captions, and related sources contain abundant implicit cues about geometry, spatial relationships, and affordances. However, this knowledge is often entangled and implicitly represented, making it difficult to retrieve for structured reasoning tasks, which leads to suboptimal performance on various spatial AI benchmarks, including ours.

Experiment Setup. We first utilize the aforementioned data

engine to construct additional instruction-tuning data that has no overlap with the testing set, ensuring a fair evaluation. We then LoRA fine-tune Qwen2.5-VL-7B using the LLaMA-Factory framework [81] on a small set of training data from one single data source or task category, and then evaluate the model’s cross-data and cross-task performance. Note that we use 800 samples for cross-task experiments and 1,200 samples per category for cross–dataset experiments. Given its limited scale, this training data is unlikely to introduce new knowledge into the MLLMs, specifically with visual encoder frozen. Instead, it primarily aims to guide the models in better utilizing the spatial knowledge already embedded within their parameters. We provide detailed training recipe in the supplementary materials.

Task-Specific Instructing Tuning. Tab. 3 presents the results of the cross-category instruction tuning experiments. Notably, using a small amount of training data from one task often leads to improvements on other tasks. This provides strong evidence that the model already possesses latent spatial knowledge, but cannot effectively leverage it through zero-shot prompting alone. Another interesting

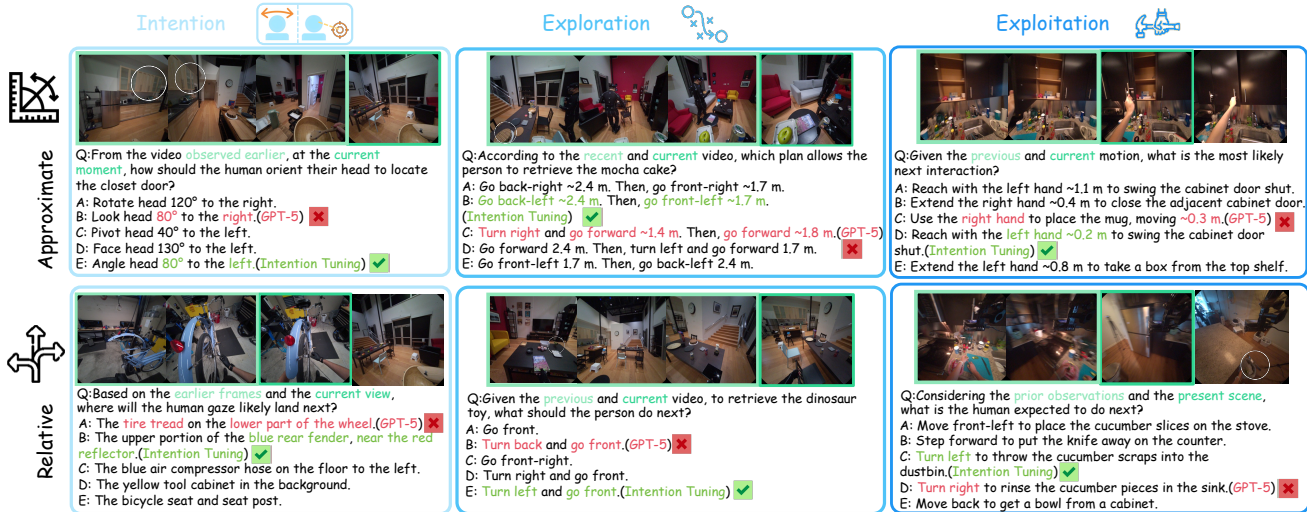


Figure 3. **Visual examples of our benchmark and model performance.** We show cases where the intention-tuned model outperforms the proprietary GPT-5 model.

observation is that although all three fine-tuning experiments use the same amount of data, the Intention training data yields a notably larger performance gain on other tasks compared to the Exploration or Exploitation training data. This aligns with our key motivation for organizing the benchmark along a cognitive hierarchy: intention provides the fundamental signals that guide both location and action. Concretely, understanding intentional cues is key to driving action-conditioned 3D reasoning, thereby providing additional insight into the instruction tuning of human-centric, 3D-aware MLLMs.

We further report model performance on the Chain-of-Actions task under task-specific tuning in Tab. 3. Both Intention tuning and Exploitation tuning lead to a slight decrease in model performance, as these data do not contain multi-step reasoning signals. In contrast, Exploration tuning, although focused primarily on navigation steps, still provides useful supervision on action locations and therefore improves multi-step reasoning. These results further confirm our hypothesis that existing MLLMs contain latent spatial intelligence, yet depend on instruction tuning to effectively express and utilize this capability.

Dataset-Specific Instructing Tuning. We conduct similar experiments under a cross-dataset setting. As shown in Tab. 4, we observe substantial performance improvements despite the large recording domain gap between ADT and EgoExo4D. Note that the improvement on the ADT Exploration task is smaller, primarily because the EgoExo4D training data do not contain any Exploration-type questions, as explained in Sec. 3.2.

5.4. Visual Illustrations

We provide visualization of the performance of GPT-5 and the instruction-tuned Qwen2.5-VL-7B (using only intention-type data) on our benchmark in Fig. 3.

GPT-5 often produces answers that appear semantically reasonable, yet it struggles with spatial reasoning, frequently failing to correctly interpret egocentric relative positions and spatial relationships. Moreover, it is unable to reliably connect cues such as spatial evidence and intention signals from the observed video to the actions that are about to occur. In contrast, the intention-tuned model consistently aligns its forecasting or planning with cues from the past video, yielding correct results. This observation also aligns with the cognitive hierarchy that motivates our benchmark design, where intention informs locomotion and reaching, and ultimately supports hierarchical interactions in complex 3D scenes. Additional visualizations and failure-case analyses are provided in the supplementary material.

6. Conclusion

In this paper, we present **EgoProx**, the first benchmark for egocentric 3D proximity reasoning. The benchmark is organized as a cognitive hierarchy with four tasks, progressing from Intention to Exploration, Exploitation, and Chain of Actions. We further introduce an agent-based data engine with a suite of tools that enables scalable and high-quality data generation. Extensive experiments reveal key spatial reasoning bottlenecks in current MLLMs. Cross-domain instruction tuning results suggest that the limited spatial understanding of MLLMs arises not from missing spatial knowledge, but from ineffective mechanisms for leveraging knowledge already encoded in model parameters.

Acknowledgments. This work was supported in part by the Zhiyuan Scholar Program from the Beijing Municipal Science and Technology Commission (Z251100008125045) and NSFC Grants.

References

- [1] Deepak Akkil, Poika Isokoski, Jani Kangas, Jussi Rantala, and Antti Oulasvirta. Gaze augmentation in egocentric video improves intention prediction. In *Proceedings of the 2016 CHI Conference on Human Factors in Computing Systems (CHI)*, pages 5181–5191, 2016. 2
- [2] Jean-Baptiste Alayrac, Jeff Donahue, Paul Luc, Antoine Miech, Iain Barr, Yana Hasson, Karel Lenc, Arthur Mensch, Katie Millican, Malcolm Reynolds, et al. Flamingo: A visual language model for few-shot learning. In *Advances in Neural Information Processing Systems (NeurIPS)*, 2022. 2, 3
- [3] Daich Azuma, Taiki Miyanishi, Shuhei Kurita, and Motoaki Kawanabe. Scanqa: 3d question answering for spatial scene understanding. *2022 IEEE/CVF Conference on Computer Vision and Pattern Recognition (CVPR)*, pages 19107–19117, 2021. 2, 4
- [4] Jinze Bai, Shuai Bai, Shusheng Yang, Shijie Wang, Sinan Tan, Peng Wang, Junyang Lin, Chang Zhou, and Jingren Zhou. Qwen-vl: A versatile vision-language model for understanding, localization, text reading, and beyond, 2023. 2, 3
- [5] Shuai Bai, Keqin Chen, Xuejing Liu, Jialin Wang, Wenbin Ge, Sibao Song, Kai Dang, Peng Wang, Shijie Wang, Jun Tang, Humen Zhong, Yuanzhi Zhu, Mingkun Yang, Zhaohai Li, Jianqiang Wan, Pengfei Wang, Wei Ding, Zheren Fu, Yiheng Xu, Jiabo Ye, Xi Zhang, Tianbao Xie, Zesen Cheng, Hang Zhang, Zhibo Yang, Haiyang Xu, and Junyang Lin. Qwen2.5-vl technical report. *arXiv preprint arXiv:2502.13923*, 2025. 6
- [6] Leonard Bärman and Alex Waibel. Where did i leave my keys? - episodic-memory-based question answering on egocentric videos. In *Proceedings of the IEEE/CVF Conference on Computer Vision and Pattern Recognition (CVPR) Workshops*, pages 1560–1568, 2022. 4
- [7] Jacob LS Bellmund, Peter Gärdenfors, Edvard I Moser, and Christian F Doeller. Navigating cognition: Spatial codes for human thinking. *Science*, 362(6415):eaat6766, 2018. 2
- [8] Boyuan Chen, Zhuo Xu, Sean Kirmani, Brain Ichter, Dorsa Sadigh, Leonidas Guibas, and Fei Xia. SpatialVlm: Endowing vision-language models with spatial reasoning capabilities. In *Proceedings of the IEEE/CVF Conference on Computer Vision and Pattern Recognition*, pages 14455–14465, 2024. 3
- [9] Sijin Chen, Xin Chen, Chi Zhang, Mingsheng Li, Gang Yu, Hao Fei, Hongyuan Zhu, Jiayuan Fan, and Tao Chen. Ll3da: Visual interactive instruction tuning for omni-3d understanding, reasoning, and planning, 2023. 3
- [10] Xi Chen, Xiao Wang, Soravit Changpinyo, Anthony J Piergiovanni, Piotr Padlewski, Daniel Salz, Sebastian Goodman, Adam Grycner, Basil Mustafa, Lucas Beyer, et al. Pali: A jointly-scaled multilingual language-image model. *arXiv preprint arXiv:2209.06794*, 2022. 2, 3
- [11] Yi Chen, Yuying Ge, Yixiao Ge, Mingyu Ding, Bohao Li, Rui Wang, Ruifeng Xu, Ying Shan, and Xihui Liu. Egoplan-bench: Benchmarking multimodal large language models for human-level planning, 2024. 3, 4
- [12] Zhe Chen, Jiannan Wu, Wenhai Wang, Weijie Su, Guo Chen, Sen Xing, Muyan Zhong, Qinglong Zhang, Xizhou Zhu, Lewei Lu, et al. Internvl: Scaling up vision foundation models and aligning for generic visual-linguistic tasks. In *Proceedings of the IEEE/CVF conference on computer vision and pattern recognition*, pages 24185–24198, 2024. 2, 3
- [13] Zhe Chen, Weiyun Wang, Yue Cao, Yangzhou Liu, Zhangwei Gao, Erfei Cui, Jinguo Zhu, Shenglong Ye, Hao Tian, Zhaoyang Liu, Lixin Gu, Xuehui Wang, Qingyun Li, Yiming Ren, Zixuan Chen, Jiapeng Luo, Jiahao Wang, Tan Jiang, Bo Wang, Conghui He, Botian Shi, Xingcheng Zhang, Han Lv, Yi Wang, Wenqi Shao, Pei Chu, Zhongying Tu, Tong He, Zhiyong Wu, Huipeng Deng, Jiaye Ge, Kai Chen, Kaipeng Zhang, Limin Wang, Min Dou, Lewei Lu, Xizhou Zhu, Tong Lu, Dahua Lin, Yu Qiao, Jifeng Dai, and Wenhai Wang. Expanding performance boundaries of open-source multimodal models with model, data, and test-time scaling, 2025. 6
- [14] Sijie Cheng, Zhicheng Guo, Jingwen Wu, Kechen Fang, Peng Li, Huaping Liu, and Yang Liu. Egothink: Evaluating first-person perspective thinking capability of vision-language models. *2024 IEEE/CVF Conference on Computer Vision and Pattern Recognition (CVPR)*, pages 14291–14302, 2023. 2, 4
- [15] Wenliang Dai, Junnan Li, Dongxu Li, Anthony Tiong, Junqi Zhao, Weisheng Wang, Boyang Li, Pascale N Fung, and Steven Hoi. Instructblip: Towards general-purpose vision-language models with instruction tuning. *Advances in neural information processing systems*, 36:49250–49267, 2023. 2
- [16] Erik Daxberger, Nina Wenzel, David Griffiths, Haiming Gang, Justin Lazarow, Gefen Kohavi, Kai Kang, Marcin Eichner, Yinfei Yang, Afshin Dehghan, et al. Mm-spatial: Exploring 3d spatial understanding in multimodal llms. In *Proceedings of the IEEE/CVF International Conference on Computer Vision*, pages 7395–7408, 2025. 3, 16
- [17] Google DeepMind. Gemini: Multimodal foundation models. *Technical Report*, 2024. 2, 3, 6
- [18] Chenyou Fan. Egovqa - an egocentric video question answering benchmark dataset. In *2019 IEEE/CVF International Conference on Computer Vision Workshop (ICCVW)*, pages 4359–4366, 2019. 4
- [19] Rao Fu, Jingyu Liu, Xilun Chen, Yixin Nie, and Wenhao Xiong. Scene-llm: Extending language model for 3d visual understanding and reasoning. *arXiv preprint arXiv:2403.11401*, 2024. 3
- [20] Kristen Grauman, Andrew Westbury, Lorenzo Torresani, Kris Kitani, Jitendra Malik, Triantafyllos Afouras, Kumar Ashutosh, Vijay Baiyya, Siddhant Bansal, Bikram Boote, Eugene Byrne, Zachary Chavis, Joya Chen, Feng Cheng, Fu-Jen Chu, Sean Crane, Avijit Dasgupta, Jing Dong, María Escobar, Cristhian Forigua, Abrahm Gebreselasie, Sanjay Haresh, Jing Huang, Md Mohaiminul Islam, Suyog Dutt

- Jain, Rawal Khirodkar, Devansh Kukreja, Kevin J Liang, Jia-Wei Liu, Sagnik Majumder, Yongsan Mao, Miguel Martin, Effrosyni Mavroudi, Tushar Nagarajan, Francesco Ragusa, Santhosh K. Ramakrishnan, Luigi Seminara, Arjun Somayazulu, Yale Song, Shan Su, Zihui Xue, Edward Zhang, Jinxu Zhang, Angela Castillo, Changan Chen, Xinzhu Fu, Ryosuke Furuta, Cristina González, Prince Gupta, Jiabo Hu, Yifei Huang, Yiming Huang, Weslie Khoo, Anush Kumar, Robert Kuo, Sach Lakhavani, Miao Liu, Romy Mi Luo, Zhengyi Luo, Brigid Meredith, Austin Miller, Oluwatumininu Oguntola, Xiaqing Pan, Penny Peng, Shraman Pramanick, Merey Ramzanova, Fiona Ryan, W. Shan, Kiran Somasundaram, Chenan Song, Audrey Southerland, Masatoshi Tateno, Huiyu Wang, Yuchen Wang, Takuma Yagi, Mingfei Yan, Xitong Yang, Zecheng Yu, Shengxin Cindy Zha, Chen Zhao, Ziwei Zhao, Zhifan Zhu, Jeff Zhuo, Pablo Arbeláez, Gedas Bertasius, David J. Crandall, Dima Damen, Jakob Julian Engel, Giovanni Maria Farinella, Antonino Furnari, Bernard Ghanem, Judy Hoffman, C. V. Jawahar, Richard A. Newcombe, Hyun Soo Park, James M. Rehg, Yoichi Sato, Manolis Savva, Jianbo Shi, Mike Zheng Shou, and Michael Wray. Ego-exo4d: Understanding skilled human activity from first- and third-person perspectives. *2024 IEEE/CVF Conference on Computer Vision and Pattern Recognition (CVPR)*, pages 19383–19400, 2023. 4, 13, 16
- [21] Yining Hong, Haoyu Zhen, Peihao Chen, Shuhong Zheng, Yilun Du, Zhenfang Chen, and Chuang Gan. 3d-llm: Injecting the 3d world into large language models. *Advances in Neural Information Processing Systems*, 36:20482–20494, 2023. 3
- [22] Zhijian Hou, Lei Ji, Difei Gao, Wanjun Zhong, Kun Yan, Chao Li, Wing-Kwong Chan, Chong-Wah Ngo, Nan Duan, and Mike Zheng Shou. Groundnlq@ ego4d natural language queries challenge 2023. *arXiv preprint arXiv:2306.15255*, 2023. 2, 3
- [23] Haifeng Huang, Yilun Chen, Zehan Wang, Rongjie Huang, Runsen Xu, Tai Wang, Luping Liu, Xize Cheng, Yang Zhao, Jiangmiao Pang, et al. Chat-scene: Bridging 3d scene and large language models with object identifiers. *Proceedings of the Advances in Neural Information Processing Systems, Vancouver, BC, Canada*, 2024. 3
- [24] Jiangyong Huang, Silong Yong, Xiaojian Ma, Xiongkun Linghu, Puhao Li, Yan Wang, Qing Li, Song-Chun Zhu, Baoxiong Jia, and Siyuan Huang. An embodied generalist agent in 3d world, 2024. 3
- [25] Junsheng Huang, Shengyu Hao, Bocheng Hu, and Gaoang Wang. Understanding dynamic scenes in ego centric 4d point clouds. *ArXiv*, abs/2508.07251, 2025. 3, 4
- [26] Shaohan Huang, Li Dong, Wenhui Wang, Yaru Hao, Saksham Singhal, Shuming Ma, Tengchao Lv, Lei Cui, Owais Khan Mohammed, Barun Patra, et al. Language is not all you need: Aligning perception with language models. *Advances in Neural Information Processing Systems*, 36:72096–72109, 2023. 2
- [27] Zeyi Huang, Yuyang Ji, Xiaofang Wang, Nikhil Mehta, Tong Xiao, Donghyun Lee, Sigmund Vanvalkenburgh, Shengxin Zha, Bolin Lai, Licheng Yu, Ning Zhang, Yong Jae Lee, and Miao Liu. Building a mind palace: Structuring environment-grounded semantic graphs for effective long video analysis with llms, 2025. 4
- [28] Baoxiong Jia, Ting Lei, Song-Chun Zhu, and Siyuan Huang. Egotaskqa: Understanding human tasks in egocentric videos, 2022. 4
- [29] Chao Jia, Yinfei Yang, Ye Xia, Yi-Ting Chen, Zarana Parekh, Hieu Pham, Quoc V Le, Yun-Hsuan Sung, Zhen Li, and Tom Duerig. Scaling up visual and vision-language representation learning with noisy text supervision. In *Proceedings of the International Conference on Machine Learning (ICML)*, 2021. 2
- [30] Robert Konrad, Nitish Padmanaban, J. Gabriel Buckmaster, Kevin C. Boyle, and Gordon Wetzstein. Gazeqpt: Augmenting human capabilities using gaze-contingent contextual ai for smart eyewear. *arXiv preprint arXiv:2401.17217*, 2024. 2, 3
- [31] Shuhe Kurita et al. Refego: Referring expression grounding in egocentric videos. In *ICCV*, 2023. 3
- [32] Bolin Lai, Xiaoliang Dai, Lawrence Chen, Guan Pang, James M Rehg, and Miao Liu. Lego: Learning ego centric action frame generation via visual instruction tuning. In *European Conference on Computer Vision*, pages 135–155. Springer, 2024. 2, 3
- [33] Hugo Laurençon et al. Idefics: An open multimodal chatbot. *Hugging Face*, 2023. 2
- [34] Feng Li, Renrui Zhang, Hao Zhang, Yuanhan Zhang, Bo Li, Wei Li, Zejun Ma, and Chunyuan Li. Llava-next-interleave: Tackling multi-image, video, and 3d in large multimodal models. *arXiv preprint arXiv:2407.07895*, 2024. 6
- [35] Junnan Li, Dongxu Li, Caiming Xiong, and Steven CH Hoi. Blip: Bootstrapped language-image pre-training for unified vision-language understanding and generation. In *Proceedings of the International Conference on Machine Learning (ICML)*, 2022. 2, 3
- [36] Junnan Li, Dongxu Li, Caiming Xiong, and Steven CH Hoi. Blip-2: Bootstrapped language-image pretraining with frozen image encoders and large language models. In *Proceedings of the IEEE/CVF Conference on Computer Vision and Pattern Recognition (CVPR)*, 2023. 2, 3
- [37] Jingli Lin, Chenming Zhu, Runsen Xu, Xiaohan Mao, Xihui Liu, Tai Wang, and Jiangmiao Pang. Ost-bench: Evaluating the capabilities of mllms in online spatio-temporal scene understanding. *ArXiv*, abs/2507.07984, 2025. 2, 4, 6
- [38] Kevin Lin et al. Egovlp: Egocentric video-language pre-training. In *NeurIPS*, 2022. 2, 3
- [39] Haotian Liu, Chunyuan Li, Qingyang Wu, and Yong Jae Lee. Visual instruction tuning. In *Advances in Neural Information Processing Systems (NeurIPS)*, 2023. 2, 3
- [40] Minghuang Ma, Haoqi Fan, and Kris M. Kitani. Going deeper into first-person activity recognition. In *Proceedings of the IEEE Conference on Computer Vision and Pattern Recognition (CVPR)*, pages 1894–1903, 2016. 2
- [41] Zongnan Ma, Jingru Men, Fuchun Zhang, and Zhixiong Nan. Egocentric intention object prediction based on a human-like manner. *Egyptian Informatics Journal*, 26:100482, 2024. 2
- [42] Arjun Majumdar, Anurag Ajay, Xiaohan Zhang, Pranav Putta, Sriram Yenamandra, Mikael Henaff, Sneha Silwal,

- Paul Mcvay, Oleksandr Maksymets, Sergio Arnaud, et al. Openeqa: Embodied question answering in the era of foundation models. In *Proceedings of the IEEE/CVF conference on computer vision and pattern recognition*, pages 16488–16498, 2024. 4
- [43] Karttikeya Mangalam, Raiymbek Akshulakov, and Jitendra Malik. Egoschema: A diagnostic benchmark for very long-form video language understanding. *ArXiv*, abs/2308.09126, 2023. 2, 4
- [44] So Yeon Min, Devendra Singh Chaplot, Pradeep Ravikumar, Yonatan Bisk, and Ruslan Salakhutdinov. Film: Following instructions in language with modular methods. *arXiv preprint arXiv:2110.07342*, 2021. 2, 3
- [45] Adrián Núñez-Marcos, Gorka Azkune, and Ignacio Arganda-Carreras. Egocentric vision-based action recognition: A survey. *Neurocomputing*, 495:28–53, 2022. 2
- [46] Takehiko Ohkawa, Takuma Yagi, Taichi Nishimura, Ryosuke Furuta, Atsushi Hashimoto, Yoshitaka Ushiku, and Yoichi Sato. Exo2egodvc: Dense video captioning of egocentric procedural activities using web instructional videos. In *2025 IEEE/CVF Winter Conference on Applications of Computer Vision (WACV)*, pages 8324–8335. IEEE, 2025. 2, 3
- [47] OpenAI. Gpt-4 technical report. *arXiv preprint arXiv:2303.08774*, 2023. 2, 3
- [48] OpenAI. Gpt-5, 2025. Accessed: 2025-08-09. 6
- [49] Xiaqing Pan, Nicholas Charron, Yongqian Yang, Scott Peters, Thomas Whelan, Chen Kong, Omkar Parkhi, Richard Newcombe, and Yuheng Carl Ren. Aria digital twin: A new benchmark dataset for egocentric 3d machine perception. In *Proceedings of the IEEE/CVF International Conference on Computer Vision*, pages 20133–20143, 2023. 4, 13, 16
- [50] Simone Alberto Peirone, Francesca Pistilli, Antonio Alliegro, and Giuseppe Averta. egovlp: Egocentric video understanding with diverse task perspectives. In *Proceedings of the IEEE/CVF Conference on Computer Vision and Pattern Recognition*, pages 18275–18285, 2024. 2
- [51] Taiying Peng, Jiacheng Hua, Miao Liu, and Feng Lu. In the eye of mllm: Benchmarking egocentric video intent understanding with gaze-guided prompting. In *Advances in Neural Information Processing Systems*, 2025. 3, 4
- [52] Shraman Pramanick, Yale Song, Sayan Nag, Kevin Qinghong Lin, Hardik Shah, Mike Zheng Shou, Rama Chellappa, and Pengchuan Zhang. Egovlpv2: Egocentric video-language pre-training with fusion in the backbone. In *Proceedings of the IEEE/CVF International Conference on Computer Vision*, pages 5285–5297, 2023. 2, 3
- [53] Zhangyang Qi, Zhixiong Zhang, Ye Fang, Jiaqi Wang, and Hengshuang Zhao. Gpt4scene: Understand 3d scenes from videos with vision-language models. *arXiv preprint arXiv:2501.01428*, 2024. 3
- [54] Alec Radford, Jong Wook Kim, Chris Hallacy, Aditya Ramesh, Gabriel Goh, Sandhini Agarwal, Girish Sastry, Amanda Askell, Pamela Mishkin, Jack Clark, et al. Learning transferable visual models from natural language supervision. In *Proceedings of the International Conference on Machine Learning (ICML)*, 2021. 2, 3
- [55] Fatemeh Shiri, Xiao-Yu Guo, Mona Golestan Far, Xin Yu, Reza Haf, and Yuan-Fang Li. An empirical analysis on spatial reasoning capabilities of large multimodal models. In *Proceedings of the 2024 Conference on Empirical Methods in Natural Language Processing*, pages 21440–21455, Miami, Florida, USA, 2024. Association for Computational Linguistics. 2
- [56] Alessandro Suglia, Claudio Greco, Katie Baker, Jose L Part, Ioannis Papaioannou, Arash Eshghi, Ioannis Konstas, and Oliver Lemon. Alanavlm: A multimodal embodied ai foundation model for egocentric video understanding. In *Findings of the Association for Computational Linguistics: EMNLP 2024*, pages 11101–11122, 2024. 2, 3
- [57] Pengzhan Sun, Junbin Xiao, Tze Ho Elden Tse, Yicong Li, Arjun Akula, and Angela Yao. Visual intention grounding for egocentric assistants, 2025. 2, 3
- [58] Quan Sun, Yufeng Cui, Xiaosong Zhang, Fan Zhang, Qiyang Yu, Yueze Wang, Yongming Rao, Jingjing Liu, Tiejun Huang, and Xinlong Wang. Generative multimodal models are in-context learners. In *Proceedings of the IEEE/CVF conference on computer vision and pattern recognition*, pages 14398–14409, 2024. 2
- [59] Ryo Suzuki, Adnan Karim, Tian Xia, Hooman Hedayati, and Nicolai Marquardt. Augmented reality and robotics: A survey and taxonomy for ar-enhanced human-robot interaction and robotic interfaces. In *CHI Conference on Human Factors in Computing Systems*, page 1–33. ACM, 2022. 2
- [60] Jianfeng Wang, Zhengyuan Yang, Xiaowei Hu, Linjie Li, Kevin Lin, Zhe Gan, Zicheng Liu, Ce Liu, and Lijuan Wang. Git: A generative image-to-text transformer for vision and language. *arXiv preprint arXiv:2205.14100*, 2022. 2
- [61] Jianyuan Wang, Minghao Chen, Nikita Karaev, Andrea Vedaldi, Christian Rupprecht, and David Novotny. Vggt: Visual geometry grounded transformer. In *Proceedings of the IEEE/CVF Conference on Computer Vision and Pattern Recognition (CVPR)*, pages 5294–5306, 2025. 3, 16
- [62] Peng Wang, Shuai Bai, Sinan Tan, Shijie Wang, Zhihao Fan, Jinze Bai, Keqin Chen, Xuejing Liu, Jialin Wang, Wenbin Ge, Yang Fan, Kai Dang, Mengfei Du, Xuancheng Ren, Rui Men, Dayiheng Liu, Chang Zhou, Jingren Zhou, and Junyang Lin. Qwen2-vl: Enhancing vision-language model’s perception of the world at any resolution, 2024. 2, 3
- [63] Ying Wang, Yanlai Yang, and Mengye Ren. Lifelongmemory: Leveraging llms for answering queries in long-form egocentric videos. *arXiv preprint arXiv:2312.05269*, 2023. 2, 3
- [64] Zehan Wang, Haifeng Huang, Yang Zhao, Ziang Zhang, and Zhou Zhao. Chat-3d: Data-efficiently tuning large language model for universal dialogue of 3d scenes. *arXiv preprint arXiv:2308.08769*, 2023. 3
- [65] Haoran Wei, Yaofeng Sun, and Yukun Li. Deepseek-ocr: Contexts optical compression, 2025. 2
- [66] Jason Wei, Xuezhi Wang, Dale Schuurmans, Maarten Bosma, Fei Xia, Ed Chi, Quoc V Le, Denny Zhou, et al. Chain-of-thought prompting elicits reasoning in large lan-

- guage models. *Advances in neural information processing systems*, 35:24824–24837, 2022. 6, 7, 13
- [67] Benita Wong, Joya Chen, You Wu, Stan Weixian Lei, Dongxing Mao, Difei Gao, and Mike Zheng Shou. Assistq: Affordance-centric question-driven task completion for egocentric assistant. In *Computer Vision – ECCV 2022*, pages 485–501, Cham, 2022. Springer Nature Switzerland. 4
- [68] Diankun Wu, Fangfu Liu, Yi-Hsin Hung, and Yueqi Duan. Spatial-mllm: Boosting mllm capabilities in visual-based spatial intelligence. *arXiv preprint arXiv:2505.23747*, 2025. 3, 16
- [69] Peiran Wu, Yunze Liu, Chonghan Liu, Miao Liu, and Junxiao Shen. St-think: How multimodal large language models reason about 4d worlds from ego-centric videos. *arXiv preprint arXiv:2503.12542*, 2025. 4
- [70] Jilan Xu, Yifei Huang, Junlin Hou, Guo Chen, Yuejie Zhang, Rui Feng, and Weidi Xie. Retrieval-augmented egocentric video captioning. In *Proceedings of the IEEE/CVF Conference on Computer Vision and Pattern Recognition*, pages 13525–13536, 2024. 2, 3
- [71] Jihan Yang, Shusheng Yang, Anjali W. Gupta, Rilyn Han, Fei-Fei Li, and Saining Xie. Thinking in space: How multimodal large language models see, remember, and recall spaces. *2025 IEEE/CVF Conference on Computer Vision and Pattern Recognition (CVPR)*, pages 10632–10643, 2024. 2, 4, 13, 16
- [72] Jingkang Yang, Shuai Liu, Hongming Guo, Yuhao Dong, Xiamengwei Zhang, Sicheng Zhang, Pengyun Wang, Zitang Zhou, Binzhu Xie, Ziyue Wang, Bei Ouyang, Zhengyu Lin, Marco Cominelli, Zhongang Cai, Yuanhan Zhang, Peiyuan Zhang, Fangzhou Hong, Joerg Widmer, Francesco Gringoli, Lei Yang, Bo Li, and Ziwei Liu. Egolife: Towards egocentric life assistant, 2025. 2, 3, 4
- [73] Sihan Yang, Runsen Xu, Yiman Xie, Sizhe Yang, Mo Li, Jingli Lin, Chenming Zhu, Xiaochen Chen, Haodong Duan, Xiangyu Yue, Dahua Lin, Tai Wang, and Jiangmiao Pang. Mmsi-bench: A benchmark for multi-image spatial intelligence. *ArXiv*, abs/2505.23764, 2025. 2, 4, 6, 16
- [74] Yuan Yao, Tianyu Yu, Ao Zhang, Chongyi Wang, Junbo Cui, Hongji Zhu, Tianchi Cai, Haoyu Li, Weilin Zhao, Zhihui He, et al. Minicpm-v: A gpt-4v level mllm on your phone. *arXiv preprint arXiv:2408.01800*, 2024. 6
- [75] Hanrong Ye, Haotian Zhang, Erik Daxberger, Lin Chen, Zongyu Lin, Yanghao Li, Bowen Zhang, Haoxuan You, Dan Xu, Zhe Gan, Jiasen Lu, and Yinfei Yang. Mmego: Towards building egocentric multimodal llms for video qa. In *International Conference on Representation Learning*, pages 71705–71723, 2025. 4
- [76] Qinghao Ye, Haiyang Xu, Jiabo Ye, Ming Yan, Anwen Hu, Haowei Liu, Qi Qian, Ji Zhang, and Fei Huang. mplug-owl2: Revolutionizing multi-modal large language model with modality collaboration. In *Proceedings of the IEEE/CVF conference on computer vision and pattern recognition*, pages 13040–13051, 2024. 2
- [77] Yuqian Yuan, Ronghao Dang, Long Li, Wentong Li, Dian Jiao, Xin Li, Deli Zhao, Fan Wang, Wenqiao Zhang, Jun Xiao, et al. Eoc-bench: Can mllms identify, recall, and forecast objects in an egocentric world? *arXiv preprint arXiv:2506.05287*, 2025. 4
- [78] Jirong Zha, Yuxuan Fan, Xiao Yang, Chen Gao, and Xinlei Chen. How to enable llm with 3d capacity? a survey of spatial reasoning in llm, 2025. 2
- [79] Yue Zhao, Ishan Misra, Philipp Krähenbühl, and Rohit Girdhar. Learning video representations from large language models. In *Proceedings of the IEEE/CVF conference on computer vision and pattern recognition*, pages 6586–6597, 2023. 2, 3
- [80] Duo Zheng, Shijia Huang, and Liwei Wang. Video-3d llm: Learning position-aware video representation for 3d scene understanding. In *Proceedings of the Computer Vision and Pattern Recognition Conference*, pages 8995–9006, 2025. 3
- [81] Yaowei Zheng, Richong Zhang, Junhao Zhang, Yanhan Ye, Zheyang Luo, Zhangchi Feng, and Yongqiang Ma. Llamafactory: Unified efficient fine-tuning of 100+ language models. In *Proceedings of the 62nd Annual Meeting of the Association for Computational Linguistics (Volume 3: System Demonstrations)*, Bangkok, Thailand, 2024. Association for Computational Linguistics. 7
- [82] Shijie Zhou, Alexander Vilesov, Xuehai He, Ziyu Wan, Shuwang Zhang, Aditya Nagachandra, Di Chang, Dongdong Chen, Eric Xin Wang, and Achuta Kadambi. Vlm4d: Towards spatiotemporal awareness in vision language models. In *Proceedings of the IEEE/CVF international conference on computer vision*, 2025. 4
- [83] Sheng Zhou, Junbin Xiao, Qingyun Li, Yicong Li, Xun Yang, Dan Guo, Meng Wang, Tat-Seng Chua, and Angela Yao. Egotextvqa: Towards egocentric scene-text aware video question answering. *2025 IEEE/CVF Conference on Computer Vision and Pattern Recognition (CVPR)*, pages 3363–3373, 2025. 2, 4
- [84] Chenming Zhu, Tai Wang, Wenwei Zhang, Jiangmiao Pang, and Xihui Liu. Llava-3d: A simple yet effective pathway to empowering llms with 3d-awareness, 2025. 3
- [85] Deyao Zhu, Jun Chen, Xiaoqian Shen, Xiang Li, and Mohamed Elhoseiny. Minigpt-4: Enhancing vision-language understanding with advanced large language models. *arXiv preprint arXiv:2304.10592*, 2023. 2

EgoProx: Evaluating MLLMs on Egocentric 3D Proximity Reasoning Across a Cognitive Hierarchy

Supplementary Material

This is the supplementary material for the paper “EgoProx: Evaluating MLLMs on Egocentric 3D Proximity Reasoning Across a Cognitive Hierarchy”. We organize the content as follows.

A – Evaluation Details

B – Benchmark Statistics

C – Implementation Details of Toolset

D – Additional Analysis on the experimental Results

E – Training Details on Domain-specific Tuning

F – Additional Visualization

G – Limitations

H – Prompt Template for Evaluation

I – Prompt Template for Training

A. Evaluation Details

General Evaluation Setup. For all evaluation processes conducted on our benchmark, we first uniformly sample each video into 8 frames. To ensure reproducibility, unless otherwise specified, we adopt a greedy decoding strategy for all models (*i.e.*, the temperature is set to 0, and both top-p and top-k are set to 1). The multimodal input to each model is formatted as follows: `[video frames] [text prompt]`. We use a unified inference prompt to ensure a fair comparison across models. The text prompt specifies the task objective and response constraints, incorporates the question text, and includes a minimal output-format exemplar to facilitate deterministic parsing during evaluation. Additionally, we append a zero-shot reasoning prefix [66] to encourage step-by-step inference behaviors commonly observed in instruction-tuned MLLMs. The exact prompt templates used for each task category are detailed in Section H.

Human Level Performance. To assess human-level performance on **EgoProx**, we adopt an evaluation procedure inspired by prior benchmarking protocols such as VSI-Bench [71]. Human participants receive both the question and its corresponding video sequence simultaneously and are allowed unlimited time to provide their responses. To conduct the evaluation, we sample a representative subset of our benchmark, selecting 50 questions per task category to ensure balanced task coverage. We recruit individuals who possess basic familiarity with spatial AI and MLLMs, and we supply clear instructions along with illustrative ex-

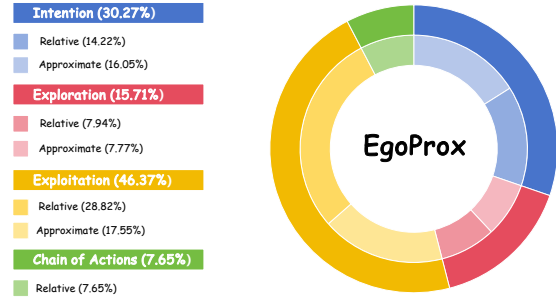


Figure 4. **Benchmark Statistics.** The distribution of tasks across four main categories in **EgoProx** with Relative and Approximate variants.

amples. Participants may replay the video as many times as needed to ensure thorough understanding of video context before making a decision.

B. Benchmark Statistics

EgoProx contains 2,405 VQA samples, encompassing a broad spectrum of egocentric 3D proximity reasoning tasks. These samples are derived from two complementary egocentric datasets: 1,016 from Aria Digital Twin (ADT)[49] and 1,389 from EgoExo4D[20]. Due to differences in dataset characteristics, task coverage varies across sources: *Exploration* tasks are exclusively generated from ADT, where locomotion is prominent, whereas *Chain of Actions* tasks rely solely on EgoExo4D, which contains dense, goal-oriented manipulation sequences. For the remaining task categories, samples are drawn from both datasets with balanced proportions.

As shown in Fig. 4, the benchmark is structured across four primary categories: *Intention* (30.27%), *Exploration* (15.71%), *Exploitation* (46.37%) and *Chain of Actions* (7.65%), reflecting the cognitive hierarchy introduced in the main paper. Except for *Chain of Actions*, each task category includes two distinct forms of proximity measurement: *Relative* and *Approximate*.

C. Implementation details of Toolset

Formally, we define the notations in Tab. 5.

C.1. Pre-Process

For the ADT dataset, we directly obtain 3D object bounding boxes \mathcal{O}^{3d} , hand skeleton positions S , eye-gaze mea-

Table 5. **Summary of input notation.** For simplicity, we omit the time step for some of the notations.

Notation	Definition
$\mathcal{X} = \{x_1, x_2, \dots, x_T\}$	Observable video segment, where T denotes the total number for frames
$\mathcal{O}^{3d} = \{o_1^{3d}, o_2^{3d}, \dots, o_N^{3d}\}$	3D object bounding boxes, where N denotes the total number of objects
E	Eye gaze data including the pose and the depth
S	Skeleton position data, including hand skeleton position
T_s^d	Transformation matrix between scene and device
T_c^d	Transformation matrix between device and camera
\hat{h}	Human-object interaction
\hat{m}	Body movement

surements E , camera poses, and egocentric video frames, and the center c_i of the objects can be calculated using the 3D bounding boxes. In contrast, the Ego-Exo4D dataset does not provide explicit 3D bounding boxes, making it difficult to localize objects in 3D space. To address this issue, we leverage the annotated interaction timestamps and approximate an object’s 3D position c_i using the mean hand-skeleton position during the corresponding interaction interval. When both hands are involved, the average position of the two hand skeletons is adopted as the proxy for the object position. Furthermore, we extract keystone information from the atomic-description annotations in the Ego-Exo4D dataset to support our downstream analysis.

C.2. Toolset for 3D Analysis

Preliminary Before introducing the proposed toolset, we outline several core definitions and notations:

1. The 3D center c_i of object i is computed as

$$c_i = \left(\frac{1}{2}(o_{i,1}^{3d} + o_{i,2}^{3d}), \frac{1}{2}(o_{i,3}^{3d} + o_{i,4}^{3d}), \frac{1}{2}(o_{i,5}^{3d} + o_{i,6}^{3d}) \right),$$

where $o_i^{3d} \in \mathbf{R}^6$ denotes the bounding-box coordinates.

2. The camera pose is represented by the transformation matrix $T_s^c = T_s^d \times T_d^c$, where

$$T = \begin{bmatrix} R & t \\ 0 & 1 \end{bmatrix}, \quad R \in \mathbf{R}^{3 \times 3}, t \in \mathbf{R}^3.$$

3. The camera center C corresponds to the translation component of T_s^c .
4. For angular reasoning in the world coordinate system, we discretize directions into eight canonical categories: *front*, *back*, *left*, *right*, *front-left*, *front-right*, *back-left*, and *back-right*.

Occupancy Map Generator The Occupancy Map Generator constructs a navigation map \mathcal{M} from the 3D bounding boxes \mathcal{O}^{3d} observed in the last frame x_T to distinguish free and occupied regions for obstacle checking. Concretely, each box is projected onto the ground plane, convex hulls are computed for the projected footprints, regions enclosed by those hulls are marked as obstacles, and the interior of the outermost hull is treated as the nominal navigable area.

Exploration Path Generator Given the goal object G and the observation video \mathcal{X} , we can compute the center c_i of G and obtain the camera center C from the camera pose in the last frame of x_T . Then the Exploration Path Generator discretizes \mathcal{M} into a 2D grid, projects the start position $p_0 = C$ and the goal position $p_K = c_i$ onto that grid, and runs an 8-connected A* search algorithm with direction-change penalties and diagonal-cut constraints to produce a feasible path. The resulting feasible path is represented as a sequence of waypoints, and each pair of adjacent waypoints defines a step \hat{s}_i . Note that we intentionally avoid using the actual human trajectory for navigation-step generation, as human motion exhibits high stochasticity and is difficult for MLLMs to reliably interpret.

Spatial Calculator The Spatial Calculator contains two subtools: the *Distance Calculator* and the *Direction Calculator*. The Distance Calculator projects the camera center C and object centers c_i into a unified world coordinate frame and computes Euclidean translation distances between queried pairs (e.g., between objects i and j). The Direction Calculator computes the angle between the camera’s forward direction and the vector from C to a target G , both projected onto the bird’s-eye-view (BEV) plane. It first extracts the camera-plane normal from T_s^c , projects both this normal vector and the vector from C to c_i into the xOy plane, and then computes the resulting angle θ .

Gaze Parser The Gaze Parser converts 2D eye-tracking points E into 3D gaze rays in the world coordinate system. These rays differ fundamentally from the camera-plane normal. For the ADT dataset, given 3D bounding boxes o_i^{3d} , the parser checks whether the gaze ray in future frames intersects any of the six faces of o_i^{3d} , while ensuring that the corresponding object appears in the last observation frame x_T . If multiple intersections exist, the closest one to the camera center is selected. For the Ego-Exo4D dataset, the parser first selects an appropriate future frame as ground truth, inserts a marker at the eye-gaze landing position, and uses an MLLM to identify the corresponding object. Using the geometric functions above, the parser returns the intentionally interacted object (and the intersection point for ADT). If a goal object is already provided, the parser instead outputs the orientation angle required to view the object.

Affordance Detector The Affordance Detector determines whether a target object will be interacted with by the observer in future frames. It operates based on three types of \hat{h} , described as follows:

- When \hat{h} is *afford*: For the ADT dataset, an object i is considered to be interacted with if at least one of the following criteria is satisfied: (1) its average velocity exceeds 0.05 m/s, or (2) the hand-skeleton position from the set of skeletons S lies inside the 3D bounding box o_i^{3d} . The average velocity is computed as the translation distance

divided by the time difference between the corresponding timestamps. For the Ego-Exo4D dataset, we pre-process the timestamps of annotated interaction keysteps. The Detector then checks whether future frames contain such keysteps and selects an appropriate future frame accordingly. After this determination, the Detector returns the direction and distance from the observer to the goal object in the last frame x_T of the observation segment \mathcal{X} , using the direction and distance computation modules described earlier.

- When \hat{h} is *place*: The Detector computes the direction from the object’s current center position c_i in the last observation frame x_T to its predicted position in the designated future frame. It additionally ensures that the placement location is visible within the observation video \mathcal{X} .
- When \hat{h} is *action*: For the Ego-Exo4D dataset, the future frame is directly provided by interaction timestamps in the annotations. The Detector uses the camera pose of the last observation frame x_T and that of the future frame to compute the turn angle within the coordinate system of the camera at x_T . The final output follows the same format as described above.

Keystep Extraction Tool The Keystep Extraction Tool returns the textual keysteps in the observation video \mathcal{X} including the interactive objects, the observer, and the interaction names from our pre-processed keystone data.

Chain Constructor The Chain Constructor obtains possible chains of steps and the direction between the steps. First, the Constructor obtains the processed textual keysteps from the Keystep Extraction. Then, it calculates the directions between the steps. More precisely, the *direction* is the direction between the adjacent pair of waypoints in the coordinate system of camera pose in the last frame x_T of the observation video. Regarding it as the basically correct chain, the tool provides several possible correct chains using multi-modal large language models.

C.3. Toolset Usage

In a nutshell, the 3D proximity ground truth for a given input clip sampled for each task type is constructed for each as follows:

- **Intention**: The agent invokes the Spatial Calculator to estimate how the camera wearer adjusts head orientation toward the goal or directs gaze, as inferred by the Gaze Parser.
- **Exploration**: The agent samples a valid goal G based on visibility checks and adopts the Occupancy Map Generator and Exploration Path Generator to obtain a path composed of steps \hat{s} including a series of waypoints, each providing the distance and discrete direction for exploration.
- **Exploitation**: The agent utilizes an affordance detector to identify which part of the object G the observer is grasping

in the anticipation frame, where the observer will place the object G , and which direction the observer will move to interact with the object G . Which of these three types is given by $\hat{h} \in \{afford, place, action\}$ specifically.

- **Chain of Actions**: Specifically, the agent employs the Keystep Extractor to extract key action steps and their 3D spatial locations from long video segments, and to identify the key actions toward the common goal G based on future observations. It then employs an LLM to construct a set of all possible ordered combinations of key steps leading toward the same goal. Finally, The agent calls the Chain Constructor to generate a complete set of possible answers by calculating the spatial relationships among the ordered combinations of key steps.

C.4. Post-Processing

The proximity measurements include both approximate transformation and relative relationships. We discretize the transformation into intervals that are interpretable by humans. For spatial relationships, we convert the 3D directions into eight discrete orientations projected onto a specified plane. When constructing the candidate sets, we prompt the VLM to generate hard-negative distraction options. However, we provide specific instructions to ensure that these distractions do not rely on minor differences that are unsolvable even for humans.

We also conduct careful human verification to ensure both the validity (whether the questioned object is visible in the video clip and whether the positions we pre-process can approximate the real coordinates), answerability (whether the questions can be answered with the provided video clips) and accuracy (correctness of the answers) of the ground truth. For the *Chain of Actions* task, we perform a thorough examination of all possible answer sets generated by the agent. To ensure that the question-answer pairs are contextually rich, accurate, and reflective of real-world egocentric interactions, we verified the data and removed the samples that failed our quality criteria, yielding the final benchmark.

D. Additional Analysis on Experiments

In this section, we provide additional analysis of the experiments conducted on our benchmark. Among the four tasks, Chain of Action poses a particularly significant challenge to existing MLLMs, especially when compared with human performance. In addition to the inherent difficulty of multi-step reasoning over extended temporal sequences, we observe that current models, especially open-source ones, struggle with instruction following when the input context becomes substantially longer. Recall that this task requires selecting from 10 candidate actions, which further increases the burden on the model’s ability to process lengthy inputs.

Regarding the other three tasks, we observe that the

Exploitation task is relatively easier for both humans and models, as it requires a much shorter temporal reasoning window. Another interesting finding is that humans are markedly better at interpreting relative spatial relationships, which naturally aligns with how people describe object locations in daily life. For existing models, estimating approximate distance appears slightly easier than identifying relative spatial relationships, since the latter requires the model to correctly infer and apply an appropriate coordinate reference.

E. Training Details on Domain-specific Tuning

For all fine-tuning experiments in this work, including the cross-category experimental setting and the cross-dataset experimental setting, we fine-tune Qwen2.5-VL-7B-Instruct with a rank-8 LoRA adapter (*target = all layers*) using the llamafactory framework. Training is performed with bfloat16 precision, AdamW optimizer, cosine learning-rate scheduling with peak learning rate 5×10^{-5} , three epochs, no warm-up, and max gradient norm 1.0. We use an effective batch size of 16 (per-device batch size of 2 with 8 gradient accumulation steps). FlashAttention is enabled automatically, and both the vision tower and multi-modal projector remain frozen.

Cross-category fine-tuning. We fine-tune the model separately using 800 training examples per category (*Intention*, *Exploration*, and *Exploitation*) generated from our Agentic Data Engine, allowing us to assess how specialization on one reasoning type transfers across others.

Cross-dataset fine-tuning. We additionally train the model using 1,200 QA samples from each source dataset: ADT [49] and EgoExo4D [20]. This setting evaluates whether dataset-specific learning improves generalization to unseen egocentric data distributions.

F. Additional Visualization

We provide additional visual examples to illustrate model behaviors across different reasoning tasks in **EgoProx**. In Fig. 5, Fig. 6, and Fig. 7, we showcase cases where the intention-tuned model generates more accurate and task-aligned answers compared to the proprietary GPT-5 model across the *Intention*, *Exploration*, and *Exploitation* task categories. These examples highlight improvements in egocentric 3D Proximity reasoning after task-aware fine-tuning.

For the *Chain of Actions* setting, Fig. 8 illustrates representative model behaviors using Gemini-2.5-Pro. Unlike the other task types, which are multiple-choice, this task requires structured reasoning: the model must generate an ordered sequence of 3–5 action steps from a set of 10 candidates and additionally infer the spatial relationship between consecutive steps. This aligns with the formula-

tion described in Sec.5.1, where an answer consists of a node sequence and corresponding spatial edges. To summarize model outcomes, we group examples into four types: fully correct (correct actions and spatial relationships), correct action sequence with spatial relationships correct under relaxed tolerance, correct action sequence but incorrect spatial relationships, and incorrect action sequence. These qualitative categories directly correspond to the quantitative metrics reported in main paper Table 2&3, namely *Act-Acc*, *Rel-Acc-S*, and *Rel-Acc-L*.

G. Limitations

A limitation of the EgoProx benchmark lies in the coverage of egocentric scenarios. Similar to most existing egocentric datasets, our current benchmark is primarily built around indoor daily activities, which means certain environments and interaction types remain underrepresented. This reflects a common bottleneck in large-scale egocentric data collection rather than a limitation of our task design. As part of future work, we plan to further diversify EgoProx by incorporating outdoor activities and other less frequent yet representative scenarios, either through new targeted data collection or through curated web-scale egocentric videos from sources such as CommonCrawl.

One limitation of our agent-based pipeline is its reliance on video metadata, such as camera pose, 3D bounding boxes, for extracting accurate 3D information. While these annotations enable precise and scalable construction of proximity ground truth, they also limit the applicability of our pipeline to datasets that provide such metadata. As future work, we plan to integrate learned 3D perception modules, for example VGGT [61], which would allow the pipeline to operate on more diverse egocentric videos without requiring pre-existing geometric annotations.

A third limitation relates to the scope of model comparisons. Following the protocol of prior Spatial AI benchmarks [71, 73], we primarily report results from prevailing general-purpose MLLMs rather than specialized spatial reasoning models. Several recent works [16, 68] have introduced architectures explicitly designed for spatial understanding, but many of these focus on generic 3D scenes or simulated environments rather than egocentric scenarios, making direct comparison less aligned with our benchmark’s goals. To maintain consistency and fairness with existing evaluation practices, we therefore do not include those models in our main results. In future work, we plan to develop more advanced spatially grounded MLLMs tailored for egocentric perception and provide comprehensive comparisons against both general-purpose and spatial-specialized models on the EgoProx benchmark.

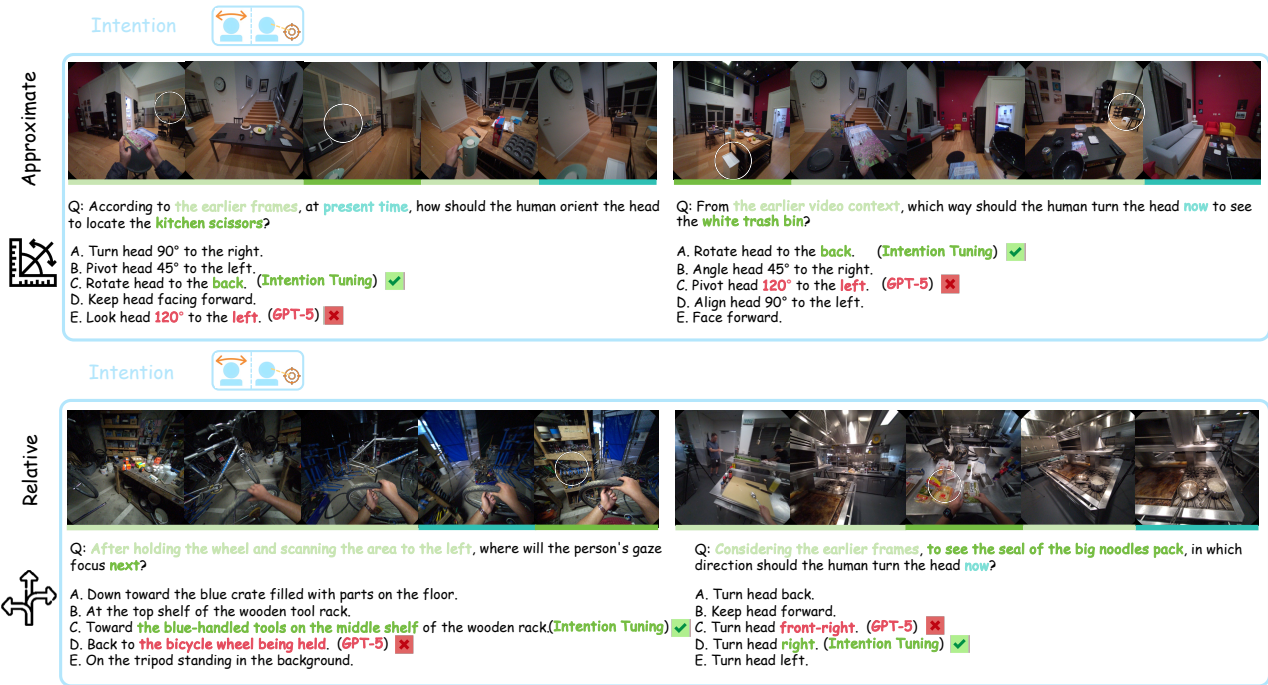


Figure 5. Visual examples of model performance on EgoProx's *Intention* task. We show cases where the intention-tuned model outperforms the proprietary GPT-5 model.

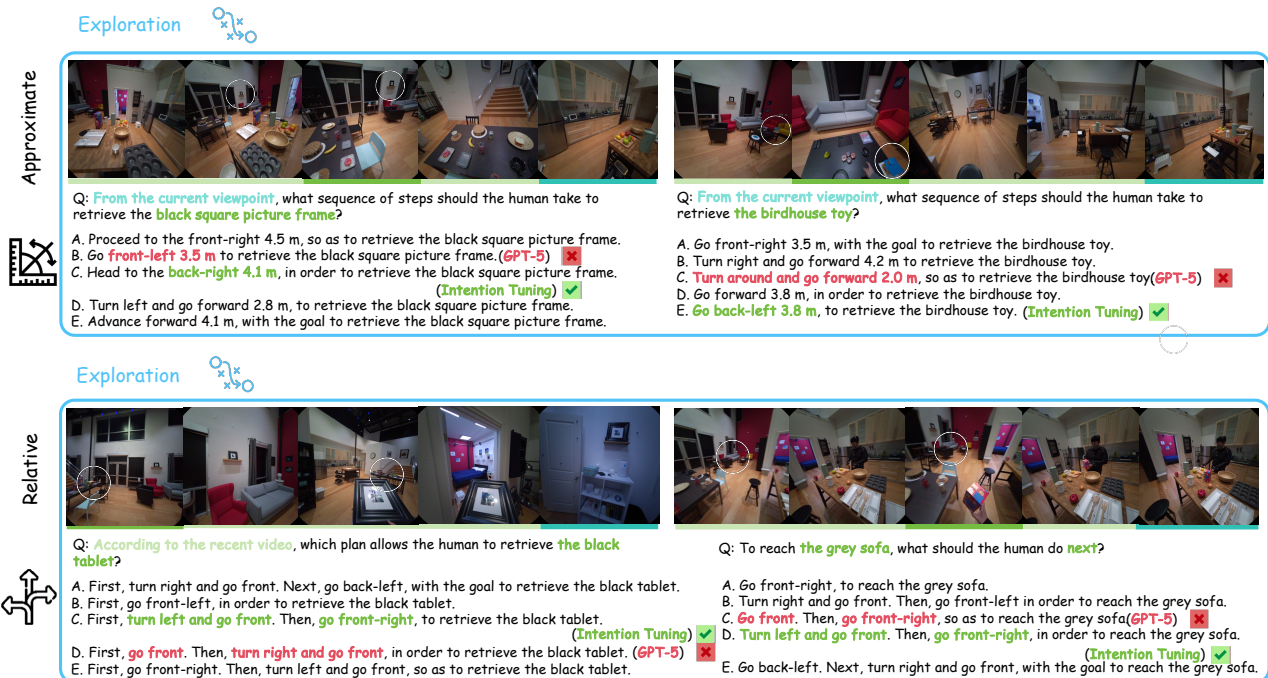


Figure 6. Visual examples of model performance on EgoProx's *Exploration* task. We show cases where the intention-tuned model outperforms the proprietary GPT-5 model.

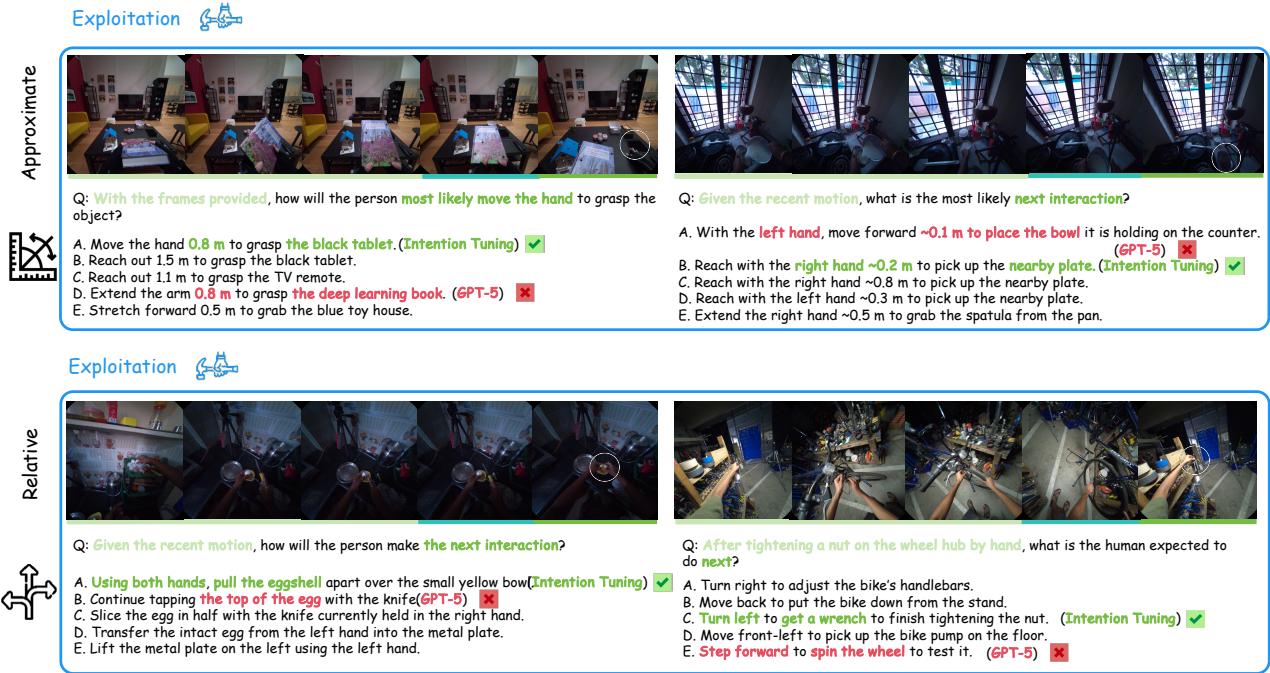


Figure 7. Visual examples of model performance on EgoProx’s Exploitation task. We show cases where the intention-tuned model outperforms the proprietary GPT-5 model.



Figure 8. Visual examples of model performance on EgoProx’s Chain of Actions task. We show representative cases illustrating the performance of Gemini-2.5-Pro.

H. Prompt Template for Evaluation

In our experiments, incorporating a chain-of-thought style prefix leads to slightly improved performance, which is consistent with findings in existing works. We further observe that providing brief examples or explicit instructions improves the parsing success rate.

For the *Intention*, *Exploration*, and *Exploitation* tasks in our **EgoProx** benchmark, we employ a unified prompt template for evaluation. In contrast, the *Chain of Actions* task differs substantially in reasoning structure and temporal planning complexity; therefore, we adopt a separate and specialized prompt template for this task. Moreover, because the *Chain of Actions* task involves varying reasoning horizons, we further provide multiple prompt variants corresponding to different action lengths.

Evaluation Prompt for *Intention, Exploration, Exploitation* Tasks in Egoprox (Without Chain-of-Thought)

System:

You are an expert in spatial reasoning, path planning, and human intention and behavior prediction. You will be given a sequence of continuous first-person video frames, a question, and multiple-choice options. The video is captured from the camera wearer's own egocentric viewpoint, meaning that "the person" or "the human" mentioned in the question refers to the camera wearer. All spatial directions (front, back, left, right, and their diagonals) are defined in this egocentric viewpoint. Your task is to analyze the visual content from this first-person perspective, reason about the scene in relation to the question, and select the correct answer from the provided options.

User:

[Frame 1]
[Frame 2]
[Frame 3]
...
[Frame 8]

Question: [Question text]

- A. [Option A text]
- B. [Option B text]
- C. [Option C text]
- D. [Option D text]
- E. [Option E text]

Choose the most appropriate option. The selected option letter in your answer must be enclosed in angle brackets (<>).

Evaluation Prompt for *Intention, Exploration, Exploitation* Tasks in Egoprox (With Chain-of-Thought)

System:

You are an expert in spatial reasoning, path planning, and human intention and behavior prediction. You will be given a sequence of continuous first-person video frames, a question, and multiple-choice options. The video is captured from the camera wearer's own egocentric viewpoint, meaning that "the person" or "the human" mentioned in the question refers to the camera wearer. All spatial directions (front, back, left, right, and their diagonals) are defined in this egocentric viewpoint. Your task is to analyze the visual content from this first-person perspective, reason about the scene in relation to the question, and select the correct answer from the provided options.

Output format: Your final line must be: The correct answer is <>.

Example:

(Reasoning...)
The correct answer is

User:

[Frame 1]
[Frame 2]
[Frame 3]
...
[Frame 8]

Question: [Question text]

- A. [Option A text]
- B. [Option B text]
- C. [Option C text]
- D. [Option D text]
- E. [Option E text]

Think step by step.

Choose the most appropriate option. The option letter in your answer should be enclosed in angle brackets (<>). Finally, end your answer with: The correct answer is <>.

Evaluation Prompt for *Chain of Actions* Task in EgoProx (Three Actions)

System:

You are an expert in continuous action planning and egocentric spatial reasoning.

You will receive:

- (1) a short first-person video segment consisting of 8 evenly sampled frames, where the last frame is the current observation;
- (2) a high-level task goal that you aim to accomplish;
- (3) a set of 10 candidate keysteps, each with an integer id;
- (4) a discrete set of 8 egocentric directions relative to the last frame:

A = right, B = left, C = front, D = back, E = front-right, F = front-left, G = back-left, H = back-right.

You should regard yourself as the camera wearer, i.e., the person whose first-person viewpoint is shown in the video.

All reasoning about space, motion, and direction must be made relative to your own egocentric viewpoint as seen in the video's last frame.

Your task:

- 1) Choose exactly three keysteps from the candidates and order them to accomplish the goal. Return their ids as [k1, k2, k3].
- 2) For each transition between consecutive keysteps (from the previous interaction to the next interaction), describe the egocentric movement direction relative to your viewpoint in the last frame. Return these as two direction letters from {A, B, C, D, E, F, G, H} for step1→step2 and step2→step3.

All directions are defined in your egocentric frame at the last frame: moving away from you is C (front), moving toward you is D (back), left/right are defined with respect to your viewpoint, and diagonals are E/F/G/H.

After completing your reasoning, directly output only the final answer in the following format (two lists, no extra text):

```
[[k1, k2, k3], [d12, d23]]
```

Example outputs:

```
[[8, 7, 3], ["F", "A"]]
```

```
[[10, 7, 9], ["E", "B"]]
```

User:

[Frame 1]

[Frame 2]

[Frame 3]

...

[Frame 8]

Goal: [Goal text]

Candidate keysteps (id: description, total = 10):

1: [Keystep 1 text]

2: [Keystep 2 text]

3: [Keystep 3 text]

...

10: [Keystep 10 text]

Egocentric direction candidates (relative to the last frame):

A: right, B: left, C: front, D: back, E: front-right, F: front-left, G: back-left, H: back-right.

Please analyze the video segment and the task goal, then provide your final answer directly in the format:

```
[[k1, k2, k3], [d12, d23]].
```

Evaluation Prompt for *Chain of Actions* Task in EgoProx (Four Actions)

System:

You are an expert in continuous action planning and egocentric spatial reasoning.

You will receive:

- (1) a short first-person video segment consisting of 8 evenly sampled frames, where the last frame represents the current observation;
- (2) a high-level task goal you aim to accomplish;
- (3) a set of 10 candidate keysteps, each with an integer id;
- (4) a discrete set of 8 egocentric directions relative to the last frame:
A = right, B = left, C = front, D = back, E = front-right, F = front-left, G = back-left, H = back-right.

You should regard yourself as the camera wearer | the person whose first-person viewpoint is shown in the video. All reasoning about space, motion, and direction must be made relative to your own body-centered frame as seen in the last frame.

Your task:

- 1) Select exactly four keysteps from the candidates and order them to accomplish the goal. Return their ids as [k1, k2, k3, k4].
- 2) For each transition between consecutive keysteps, describe the egocentric movement direction relative to the last frame. Return these as [d12, d23, d34], where each direction is a single letter from {A{H}}.

All directions are defined relative to your egocentric viewpoint in the last frame: moving away from you corresponds to C (front), moving toward you corresponds to D (back), left/right are determined by your viewpoint, and diagonal movements map to E/F/G/H.

After reasoning, output only the final result in the following format (two lists, no explanation or additional text):

```
[[k1, k2, k3, k4], [d12, d23, d34]]
```

Example outputs:

```
[[8, 7, 3, 9], ["F", "A", "H"]]  
[[10, 7, 9, 8], ["E", "B", "A"]]
```

User:

```
[Frame 1]  
[Frame 2]  
[Frame 3]  
...  
[Frame 8]
```

Goal: [Goal text]

Candidate keysteps (id: description, total = 10):

```
1: [Keystep 1 text]  
2: [Keystep 2 text]  
3: [Keystep 3 text]  
...  
10: [Keystep 10 text]
```

Egocentric direction candidates (relative to the last frame):

A: right, B: left, C: front, D: back, E: front-right, F: front-left, G: back-left, H: back-right.

Please analyze the scene and provide your final answer directly in the format:

```
[[k1, k2, k3, k4], [d12, d23, d34]].
```

Evaluation Prompt for *Chain of Actions* Task in EgoProx (Five Actions)

System:

You are an expert in continuous action planning and egocentric spatial reasoning.

You will receive:

- (1) a short first-person video segment consisting of 8 evenly sampled frames, where the last frame represents the current observation;
- (2) a high-level task goal you aim to accomplish;
- (3) a set of 10 candidate keysteps, each with an integer id;
- (4) a discrete set of 8 egocentric directions relative to the last frame:
A = right, B = left, C = front, D = back, E = front-right, F = front-left, G = back-left, H = back-right.

You should regard yourself as the camera wearer | the person whose first-person viewpoint is shown in the video. All reasoning about space, motion, and direction must be made relative to your own egocentric viewpoint as seen in the last frame.

Your task:

- 1) Select exactly five keysteps from the candidates and order them to accomplish the goal. Return their ids as [k1, k2, k3, k4, k5].
- 2) For each transition between consecutive keysteps, describe the egocentric movement direction relative to the last frame. Return these as [d12, d23, d34, d45], where each direction is a single letter from {A{H}.

All directions are defined relative to your egocentric viewpoint in the last frame: moving away from you corresponds to C (front), moving toward you corresponds to D (back), left/right are determined by your viewpoint, and diagonal movements map to E/F/G/H.

After reasoning, output only the final result in the following format (two lists, no explanation or additional text):

```
[[k1, k2, k3, k4, k5], [d12, d23, d34, d45]]
```

Example outputs:

```
[[8, 7, 3, 4, 5], ["F", "A", "E", "B"]]  
[[10, 7, 9, 6, 8], ["E", "B", "D", "C"]]
```

User:

```
[Frame 1]  
[Frame 2]  
[Frame 3]  
...  
[Frame 8]
```

Goal: [Goal text]

Candidate keysteps (id: description, total = 10):

```
1: [Keystep 1 text]  
2: [Keystep 2 text]  
3: [Keystep 3 text]  
...  
10: [Keystep 10 text]
```

Egocentric direction candidates (relative to the last frame):

A: right, B: left, C: front, D: back, E: front-right, F: front-left, G: back-left, H: back-right.

Please analyze the scene and provide your final answer directly in this format:

```
[[k1, k2, k3, k4, k5], [d12, d23, d34, d45]].
```

I. Prompt Template for Training

LoRA Instruction-Tuning Prompt in EgoProx

System:

You are an expert in spatial reasoning, path planning, and human intention and behavior prediction. You will be given a sequence of continuous first-person video frames, a question, and multiple-choice options. The video is captured from the camera wearer's own egocentric viewpoint, meaning that "the person" or "the human" mentioned in the question refers to the camera wearer. All spatial directions (front, back, left, right, and their diagonals) are defined in this egocentric viewpoint. Your task is to analyze the visual content from this first-person perspective, reason about the scene in relation to the question, and select the correct answer from the provided options.

User:

[Frame 1]
[Frame 2]
[Frame 3]
...
[Frame 8]

Question: [Question text]

- A. [Option A text]
- B. [Option B text]
- C. [Option C text]
- D. [Option D text]
- E. [Option E text]

Choose the most appropriate option. The option letter in your answer should be enclosed in angle brackets (<>).

Assistant:

The correct answer is <[Option Letter]>: [Chosen option text].